Universidade de Aveiro Departamento de Química
Ano 2013

VANESSA RITA FONSECA AUGUSTO

Perfil lipídico de macrófagos infectados com *Leishmania infantum*

Lipid profile of *Leishmania infantum* infected macrophages

Universidade de Aveiro Departamento de Química
Ano 2013

VANESSA RITA FONSECA AUGUSTO

Perfil lipídico de macrófagos infectados com *Leishmania infantum*

Lipid profile of *Leishmania infantum* infected macrophages

Dissertação apresentada à Universidade de Aveiro para cumprimento dos requisitos necessários à obtenção do grau de Mestre em Bioquímica, ramo da Bioquímica Clínica realizada sob a orientação científica da Doutora Maria do Rosário Gonçalves dos Reis Marques Domingues, professora auxiliar do Departamento de Química da Universidade de Aveiro, Doutora Anabela Cordeiro da Silva, Professora associada da Faculdade de Farmácia Universidade do Porto/ IBMC e Doutor Bruno Miguel Rodrigues das Neves, professor auxiliar convidado do Departamento de Química da Universidade de Aveiro.

Thanks are due to Portuguese Foundation for Science and Technology (FCT), European União, QREN, and COMPETE for funding the QOPNA research unit (project PEst-C/QUI/UI0062/2013), and the research project (PTDC/BIA-MIC/118644/2010)

Dedico este trabalho à minha mãe, irmão e Tiago pelo incansável apoio.

o júri

presidente

Prof. Doutora Rita Maria Pinho Ferreira
professora auxiliar convidada do Departamento de Química da Universidade de Aveiro

Prof. Doutora Maria Teresa Teixeira da Cruz Rosete
professora auxiliar da Faculdade de Farmácia da Universidade de Coimbra

Prof. Doutora Maria do Rosário Gonçalves Reis Marques Domingues
professora auxiliar do Departamento de Química da Universidade de Aveiro

Prof. Doutora Anabela Cordeiro da Silva
Professora associada da Faculdade de Farmácia Universidade do Porto/ IBMC

Prof. Doutor Bruno Miguel Rodrigues das Neves
professor auxiliar convidado do departamento de Química da Universidade de Aveiro

Agradecimentos

Gostaria de agradecer em primeiro lugar aos meus orientadores Professora Rosário Domingues, Professora Anabela Cordeiro e Professor Bruno Neves pelos seus ensinamentos, orientação, disponibilidade, motivação ao longo do trabalho, oportunas sugestões e confiança depositada.

Ao grupo do laboratório de espectrometria de massa em especial, à Deolinda, Tânia, Beta, Luísa e Edgar por toda ajuda, ensinamentos, conselhos e boa disposição.

A todos os meus amigos em especial ao Tiago, Carlos, David, Ana, Stéphanie, Maria, Hugo, João, Inês, Sara, Diana e Vítor pela paciência, apoio e pelos momentos de descontração.

Por fim, quero agradecer à minha mãe, Graça e ao meu irmão, Leandro pelo apoio, carinho, motivação e confiança que depositaram em mim.

palavras-chave

Leishmania, leishmaniose visceral, macrófagos, resposta imunológica, interação macrófago-*Leishmania* e lipidómica.

resumo

A leishmaniose visceral (LV) é uma doença infeciosa causada por algumas espécies do género *Leishmania* (*L. infantum* e *L. donovani*) que se revela particularmente problemática nas regiões tropicais e subtropicais. Uma vez no hospedeiro, os parasitas apresentam um grande tropismo para os macrófagos subvertendo as funções imunomoduladoras destas células. O estudo destes mecanismos de subversão foi durante largos anos focado na modulação a nível proteico, sendo dada pouca relevância ao efeito dos parasitas no perfil lipídico dos macrófagos. No entanto, devido ao crescente conhecimento acerca das funções imunomoduladoras dos lípidos, estes podem ser vistos como alvos terapêuticos promissores para o tratamento da leishmaniose. Deste modo, o objetivo geral deste trabalho consistiu na análise do perfil lipídico de macrófagos infectados com *Leismania infantum*, usando uma abordagem lipidómica, de modo a elucidar a contribuição de mudanças induzidas na patogénese da infeção. As diferentes classes de fosfolípidos foram separadas por TLC e quantificadas por através de um ensaio de fósforo e os ácidos gordos analisados por GC-FID. O extrato lipídico total foi analisado por espetrometria de massa de cromatografia líquida de alta eficiência (HPLC-MS e MS / MS), permitindo a identificação da estrutura detalhada dos fosfolípidos, nomeadamente da cabeça polar e composição dos ácidos gordos. O perfil fosfolipídico dos macrófagos revelou ser notoriamente alterado após a infeção tendo-se observado uma diminuição significativa no teor de PC e um correspondente aumento no conteúdo de LPC apenas em células infectadas com promastigotas viáveis. Verificou-se ainda que a infeção com parasitas viáveis causou uma diminuição no teor relativo de ácido palmítico e um aumento na razão de ácidos gordos C18/C16. Os resultados de HPLC-MS reforçaram estas observações, tendo evidenciado alterações consideráveis nos perfis de PC, LPC, PI e PS entre macrófagos, macrófagos expostos a promastigotas mortos ou viáveis. Avaliada a transcrição de genes relacionados com o metabolismo lipídico verificou-se um aumento nos níveis de ARNm dos genes *Pla2gaf*, *Fabp4* e *Elovl2,* podendo justificar deste modo os aumentos previamente observados nos níveis de LPC e ácidos gordos C18. Por fim observou-se que os promastigotas possuem considerável atividade enzimática PLA_2 e que esta atividade poderá estar relacionada com a entrada do parasita na célula facilitando a infeção.

keywords *Leishmania*,visceral leishmaniasis, macrophages, immune response, interaction macrophage-Leishmania, and lipidomics.

abstract Visceral leishmanisis (VL) is an infectious disease caused by protozoan parasites of the genus *Leishmania* (*L. infantum* and *L. donovani)* that raises great concerns particularly in tropical and subtropical regions. Once in the host, parasites have a tropism to macrophages and actively subvert the immunomodulatory functions of these cells. Little attention was put on the effect of parasites on macrophage's lipid profile. However, due to the lipids biological significance they can be viewed as a promising therapeutic target for the treatment of leishmaniasis. Therefore, the general aim of this work is to use a lipidomic approach to analyze the lipidomic profile of Leishmania infantum infected macrophages in order to elucidate the contribution of induced changes in the pathogenesis of this infection. For this purpose, the different classes of phospholipids were separated by TLC and quantified by a phosphorous assay and the fatty acids were analyzed by gas chromatography with a flame ionization detector (GC-FID). The total lipid extract was analyzed by high-performance liquid chromatography mass spectrometry (HPLC-MS and MS/MS), allowing the identification of the detailed structure of phospholipids, namely the polar head and fatty acid composition. The phospholipid profile of macrophages was found to be markedly altered after infection since a significant decrease in the content of PC and a corresponding increase in the content of LPC were observed only in cells infected with promastigotes. Furthermore, it was also observed that infection with viable parasites caused a decrease in relative content of palmitic acid and an increase in the ratio of C18/C16 fatty acids. The results of HPLC-MS supported these findings and showed considerable changes in the profiles of PC, LPC, PI and PS between macrophages, macrophages exposed to viable or fixed promastigotes. The evaluation of the transcription of genes related to lipid metabolism showed an increase in mRNA levels of genes *Pla2gaf*, *Fabp4* and *Elovl2* thereby supporting the previous results regarding the increase in LPC levels and the increase of C18 fatty acids. Finally we found that promastigotes have considerable PLA_2 enzyme activity and that this activity may be related to the parasite entry in the cell facilitating infection.

Index

Figures index

Tables index

Abbreviations

β-MCD: β-methyl-cyclodextrin

AIDS- acquired immunodeficiency syndrome

AP-1- activator protein 1

C- carbon

CER- ceramide

Cl- cutaneous leishmaniasis

CL- cardiolipin

COX- cyclooxygenas

DAG- diacylglycerol

DAT- Direct agglutination test

DENV- Dengue virus

DNA- deoxyribonucleic acid

ELISA- enzyme-linked immunosorbent assay

ERK- extracelular signal-regulated kinases

FA- fatty acid

FAZ- fatty acid synthase

GC- gas chromatography

GIPL- glycosylinositophospholipid

GL- glycerophospholipid

GPI- glycosylphosphatidylinositol

H_2O_2- Hydrogen peroxide

HCV- Hepatite C virus

PA- phophatidic acid

HPLC- high-performance liquid chromatography

IFAT- indirect fluorescence antibody technique

ICT- immunochromatographic test

IL- interleukine

IFNγ- interferon gama

JAK- janus kinase

JNK- c-Jun N-terminal kinase

LC- liquid chromatography

LPC- lysophosphatidylcholine

LPG- lipophosphoglycan

LPL- lysophospholipids

LPS- Lipopolysaccharide

MAP- mitogen-activated protein

MS- mass spectrometry

MUFA- mono-unsaturated fatty acid

NF-κB- factor nuclear kappa B

NMR- nuclear magnetic resonance

NO- nitric oxide

O_2^{-}- superoxide

OBBA- 3-(4-octadecyl-benzoylacrylic acid)

$OH^{\cdot}$- hydroxyl radical

PC- Phosphatidylcholine

PCR- polymerase chain reaction

PE- phosphatidylethanolamine

PG- phosphatidylglycerol

PKC- protein kinase C

PLA_2- phospholipase A_2

PPG- proteophosphoglycan

PS- phosphatidylserine

PTB1B- Protein tyrosine phosphatase 1B

PUFA- poly-unsaturated fatty acid

PV- parasitophorous vacuoles

RAGER- receptor for advanced glycosilaton products

RNS- reactive nitrogen specie

ROS- reactive oxygen specie

RT-PCR- Reverse transcription polymerase chain reaction

SAP- secreted acid phosphatase

SFA- saturated fatty acid

SL- sphingolipid

SM- sphingomyelin

SMS- sphingomyelin synthase

STAT- Signal Transducer and Activator of Transcription

TCPTP- T-Cell Protein Tyrosine Phosphatase

Th- T helper

TF- transcription factor

TLC- thin-layer chromatography

TNFα- tumor necrose factor alpha

Tyr- Tyrosine

Tyk- tyrosine kinase

UFA- unsaturated fatty acid

VL- visceral leishmaniasis

WB-western blotting

WHO-world health organization

I. Introduction

I.Introduction

1. Introduction

Protozoan parasites of *Leishmania* genus are the etiological agents of human diseases in tropical and subtropical countries and also in more temperate regions such the Mediterranean basin. Multiple species of *Leishmania* are known to infect humans causing diseases that manifest as cutaneous and diffuse cutaneous leishmaniasis; mucocutaneous or visceral leishmaniasis (1–5). *Leishmania* parasites are usually transmitted by the bite of infected female sandflies (of the genus *Phlebotomus* in the Old World and the genus *Lutzomyia* in the New World), which inoculates mammalian hosts. Mammalian infection starts when the sandflies during a blood feeding, release the flagellated promastigote form of the parasite into the host. There, parasites are rapidly taken up by phagocytic cells (e.g. neutrophils, macrophages and immature dendritic cells) and differentiate into the replicative and aflagellated form termed amastigote (1,5–7). Clinical manifestations of leishmaniasis are dependent of the immunological status of the host, *Leishmania*'s specie and the localization of parasite in cutaneous tissues or internal organs of the host (2,8). The epidemiology is very diverse: 20 *Leishmania* species are pathogenic for humans and 30 sandflies species are proven vectors (9). Cutaneous leishmaniasis (Cl) is caused by *L. major*, *L. tropica*, *L. mexicana*, and *L. braziliensis* and is characterized by a transient skin lesion (papule or ulcer) at the site of the insect bite. These lesions are normally painless and often spontaneously self-heal but when the lesions are multiple, Cl become disabling and disfiguring (7,9). Diffuse Cl represents the rarest and more severe cutaneous manifestation and occurs in individuals with defective cell-mediated immune response, being very difficult to treat. The lesions caused by this infection are similar of those caused by lepromatous leprosy. Mucocutaneous leishmaniasis is primarily caused by *L. braziliensis* and leads to extensive destruction of naso-oropharyngeal cavities with disfiguring lesions, mutilation of the face and great suffering for life (7,9). Visceral leishmaniasis (VL), also known as kala-azar is caused by *L. infantum* and *L. donovani* and is often fatal if untreated. The clinical manifestations of this disease includes: fever, abdominal discomfort, weight loss, pallor, splenomegaly and hepatomegaly (9,10).

The World Health Organization (WHO) reports that leishmaniasis is still one of the world's most neglected diseases, affecting mainly the poor population of developing countries. It is estimated that 350 million in 80 countries people are at risk of contracting leishmaniasis, and that approximately 2 million new cases occur every year (8). In the last decade, important scientific discoveries have been made in the treatment, diagnosis and prevention of leishmaniasis. Thus, measures such as the control of reservoirs hosts and vectors, early diagnosis and an efficient treatment are crucial to handle this infection (8). For more than half century, pentavalent antimonials have been used as first–line pharmacological approaches for VL treatment, however, currently these compounds has been replaced by amphotericin B and miltefosine (11,12). A human anti-leishmanial vaccine is not available, therefore the control of the disease depends on prophylaxis and chemotherapy. However, the drugs available for the treatment of leishmaniasis have several disadvantages such as: toxicity, expensive cost and they are associated to an increase resistance. The development of new drugs to avoid the disadvantages referred above and the development of a immunoprotective vaccine is an enormous challenge due to the different forms of leishmaniasis, variety of parasite species, pathology and complexity of the immune response associated to these infections (8). Therefore, a better understanding of the evasion/subversion mechanisms used by *Leishmania* parasites to escape immune system could identify new therapeutic targets and be a great help to develop more efficient anti-leishmanial therapies in the future.

2. *Leishmania* life cycle

During its life cycle, *Leishmania* acquires two distinct morphological forms: the flagellated elongated promastigote and the aflagellated spherical amastigote (1,13,14). The parasite life cycle starts when sandflies belonging to the genera *Phlebotomus* or *Lutzomyia* take a blood meal from a mammalian host and ingest infected cells containing amastigotes. After the vector's blood meal, the amastigote transforms into a promastigote in the gut of the insect. If the insect is an appropriate vector, the promastigote attaches to the midgut epithelium, otherwise the organism is eliminated by the insect's gut. While attached to the gut, the promastigotes multiply by longitudinal binary fission. When the sandfly feeds again, the infective metacyclic promastigotes detach from the gut wall of the insect and are injected in the mammalian host (15,16) . The promastigotes are then phagocytized by

macrophages within minutes, being this internalization process facilitated by complement receptor-mediated recognition of surface bound C3b and/or C3bi opsonins (17). Promastigotes are internalized into phagosomes that fuse with lysosomes to become phagolysosomes, structures that in this particular infection are referred as parasitophorous vacuoles (PV). Once inside host cells, promastigotes suffer a morphological and structural transformation becoming the intracellular aflagellated form of the parasite, termed amastigote (figure 1). The reproduction of amastigotes in the macrophages ultimately ruptures cells and thus spread the infection (1,14). Factors such as the species of *Leishmania* involved, temperature, immune system of the host, and even behavioral characteristics of the insect vector may determine the extent and site of infection in the mammalian host (14–16). A critical point for the *Leishmania* infection outcome is the interaction of parasites with macrophages, which is mainly drive by the surface molecules of the parasite. The surface of the *Leishmania* has a wide variety of important molecules for the evasion and survival of the parasite into phagocytic cells during the infection, including: lipophosphoglycan (LPG), glycosylphosphatidylinositol (GPI)–anchored molecules, and glycosylinositophospholipids (GIPLS) (3,13,18).

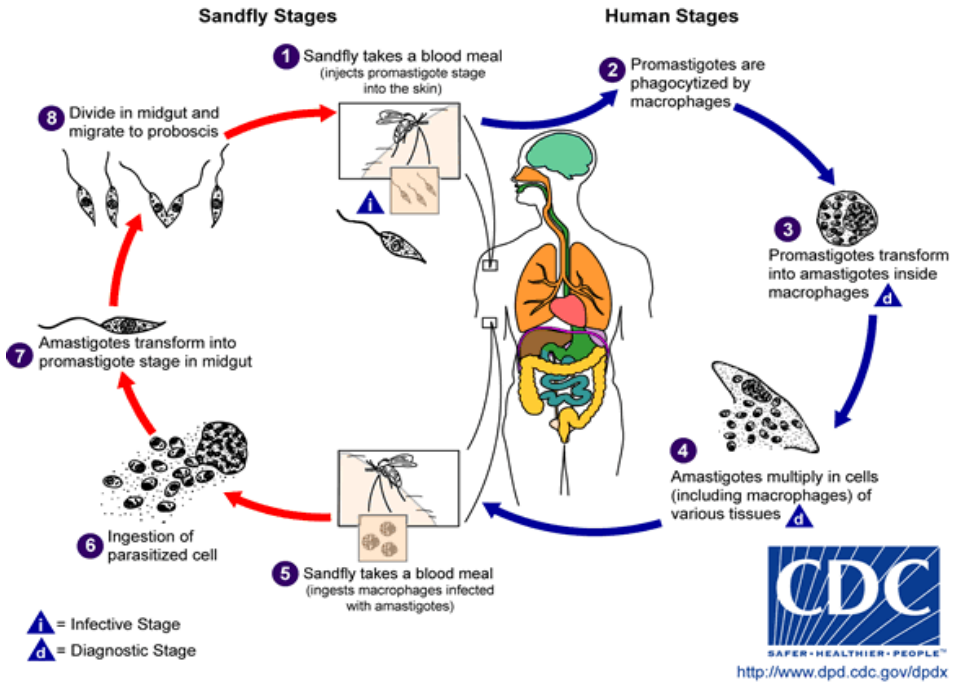

Figure 1: *Leishmania* life cycle. Representation of the main *Leishmania* developmental stages: the sandfly stage involves the entry of the parasites into the mosquito after a blood meal and its transformation in the promastigote form in the midgut of the sandfly; the mammalian stage represents the phagocytosis of the promastigote form of the parasites by macrophages after the sandfly bite. In the macrophages the promastigotes will transform in the infectious amastigote form, thus spreading the infection. Image taken from Centers for Disease Control and Prevention (CDC) (19).

2.1 *Leishmania* virulence factors

As referred above, *Leishmania* parasites have complex strategies to survive, being many of them intimately related to evasion of host immune response. This ability is due to specific *Leishmania* structures that play an important role in the steps required for a successful infection. These structures are considered virulence factors and include among others, cell surface glycoconjugates such as: lipophosphoglycans (LPGs), glycosilinositolphospholipids (GIPLs), GPI-anchored molecules and proteophosphoglycans (PPGs); secreted acid phosphatases and a vast arsenal of proteases (Figure 2).

LPG represents the major cell surface glycoconjugate of promastigotes presenting a conserved glycan core region of Gal(α1,6)Gal(α1,3)Galf(β1,3)[Glc(α1)-PO_4]-Man(α1,3)Man(α1,4)-GlcN(α1) linked to a 1-O-alkyl-2-lyso-phosphatidylinositol anchor. Structure differs however, between *Leishmania* species in the sugar composition and

sequence of branching sugars attached to the repeat units and cap structure (20–22). In the last 20-30 years, enormous effort has been made in order to elucidate the role of LPG in *Leishmania* biology and virulence. Thus, LPG has been related to the inhibition of protein kinase C (PKC) (23), arresting of phagosome maturation (24), *Leishmania* parasites infectivity (25) and to the blockade of NADPH oxidase (26). One of the first reports on specific effects of LPG showed that purified *L. donovani* parasites turned macrophages unresponsive to stimulations with LPS and PKC inducers. This effect was related to the potent *L. donovani* LPG PKC inibithory activity observed *in vitro* (23). Furthermore, it has also been reported that LPG inhibits phagosome maturation in the early stage of infection, allowing promastigotes to survive inside the vacuole (24) and that LPG blocks NADPH oxidase assembly at the phagosome membrane (26). Regarding the effect of LPG in the parasite infectivity, several studies showed that *L. major* promastigotes lacking the lpg1 gene thus, lacking LPG but containing normal levels of related glycoconjugates, caused a greatly attenuated infection. However, parasite virulence was restored when lpg1 gene was reintroduced (25). Others parasite cells surface glycoconjugates important for its successful infection are the GIPLs. The basic structure of GIPLs is a Manα1-4GlcN linked to an alkyl-acylglycerol through a phosphatidylinositol (PI) residue. This molecule family is divided into type-I GIPLs, type-II GIPLs and hybrid-type GIPLs based on their fatty acid substitutions in the lipid anchor and monosaccharide substitutions in the glycan core moiety (27). Recent findings demonstrated that *L.braziliensis* GIPLs are components of complex membrane microdomains and that these molecules were necessary for the parasite survival and infectivity (27,28). Furthermore, it has been reported that *Leishmania* GIPLs were also very effective in inhibiting PKC activity (29). GPI-anchored molecules are also implicated in the parasite survival since they play a key role in cell signaling and act as agonists and second messengers in response to cytokines and others stimuli (27,30,31). GPIs share a common core consisting of ethanolamine-PO_4-6Manα1-2Manα1-6Manα1-4GlcNα1-6myo-Ino-1-PO_4-lipid (32) . In addition to the glycoconjugates mentioned above, the PPGs also seem to be involved in the establishment of *Leishmania* infection. PPGs can take various forms going from filamentous (fPPGs), secreted (sPPGs) to membrane bound (mPPGs) components (33). It has been shown that sPPG isolated from *L. major* promastigote cultures interacts with murine macrophages blocking LPS-induced TNFα secretion (33). However, another study reported that sPPG synergistically increase IFNγ-

stimulated NO production, suggesting a duality of sPPG in inflammatory responses (34). The proteophosphoglycan Promastigote Secretory Gel (PSG) also seem to favor the parasite infection since it participates in the *Leishmania* transmission by blocking the lumen of the insect's anterior midgut and stomodeal valve, resulting in a regurgitation of metacyclic promastigotes during bloodmeal (35,36)

Secreted acid phosphatases (SAPs) are part of the surface of all species of *Leishmania* studied to date. Considering that SAPs have several substrates including: phosphorylated sugars, inositol phosphates, phosphorylated proteins and that they have a preference for acidic pH, it has been suggested that these enzymes modulate host environment and provide nutrients for the parasites (37).

One of the most studied *Leishmania* virulence factor is the metalloprotease GP63. This protease is involved in several strategies employed by *Leishmania* parasites to escape and subvert the immune system in order to survive and spread the infection. It was shown to be essential to the Leishmania´s resistance to the phagolysosome acidic and hydrolase-rich environment (33). GP63 is a zinc-dependent metalloprotease belonging to the metzincin class whose members share a similar sequence motif HExxHxxGxxH, and an N-terminal pro-peptide. This metalloprotease is more abundant in promastigotes, however the absence of LPG in the amastigote surface makes that GP63 play an important role in the ability of amastigotes to modulate the host immunity despite its lower expression compared to promastigotes (33). It has been shown that proteins entrapped in liposomes are protected from phagolysosomal degradation when coated with purified *L. mexicana* GP63 and that this protection is lost when GP63 is destroyed by heat denaturation. Therefore, this data provides indirect evidence about the protective role played by GP63 towards *Leishmania* amastigotes (38). Similarly, Chen and collaborators demonstrated that reduced GP63 levels by expression using specific antisense RNAs in *L. amazonensis* promastigotes decreases their intracellular survival rate (39). These findings suggest that GP63 is crucial for the protection of intracellular amastigotes from the severe environment of phagolysosome. Furthermore, GP63 represent the most abundant protein in *Leishmania* vesicles, which are related to death inducing stimuli (40).

GP63 is also directly involved in the *Leishmania*'s capacity to exploit phosphatases as negative regulators of intracellular signaling cascades. It has been reported, using an *L.*

major strain deficient in GP63, that this metalloprotease was effectively responsible for the activation of SHP-1, PTB1B and TCPTP and that the activation of these majors protein tyrosine phosphatases (PTPs) was done by cleavage in their C_0 terminal portion (41). The *Leishmania* virulence factor GP63 also seems to directly modulate transcription factors crucial to several macrophage functions, such as AP-1 and NF-κB (33,42,43). The transcription factor AP-1, important in IFNα-induced NO production, is formed by homodimers of Jun family members (c-Jun, JunB and Jun D), or heterodimers of Jun and Fos family members (c-Fos, Fos B, Fra 1 and Fra 2) (33). It was showed that GP63 is able to reach the nuclear compartment where it degrades and cleaves c-Jun and other AP-1 subunits and therefore drastically affect the integrity of the transcription factor AP-1 during the early stage of *Leishmania* infection (44). The NF-κB is related with gene expression involved in a wide range of macrophage functions, being a master regulator of innate immune response. Gregory and colleagues reported that several *Leishmania* species infect macrophages and effectively induce the specific cleavage of the NF-κB p65RelA subunit in the cytoplasm (42). This cleavage was shown to be critical for the selective induction of cytokines and chemokines by *Leishmania*-infected macrophages. Furthermore, the NF-κB family also seems to influence the host cell cytokine production of human phagocytes infected by *Leishmania* parasites (43).

These findings demonstrated that the metalloprotease GP63 represents an important virulence factor since it's related with several alterations of host immune cells, thus favoring *Leishmania* survival and infection progression.

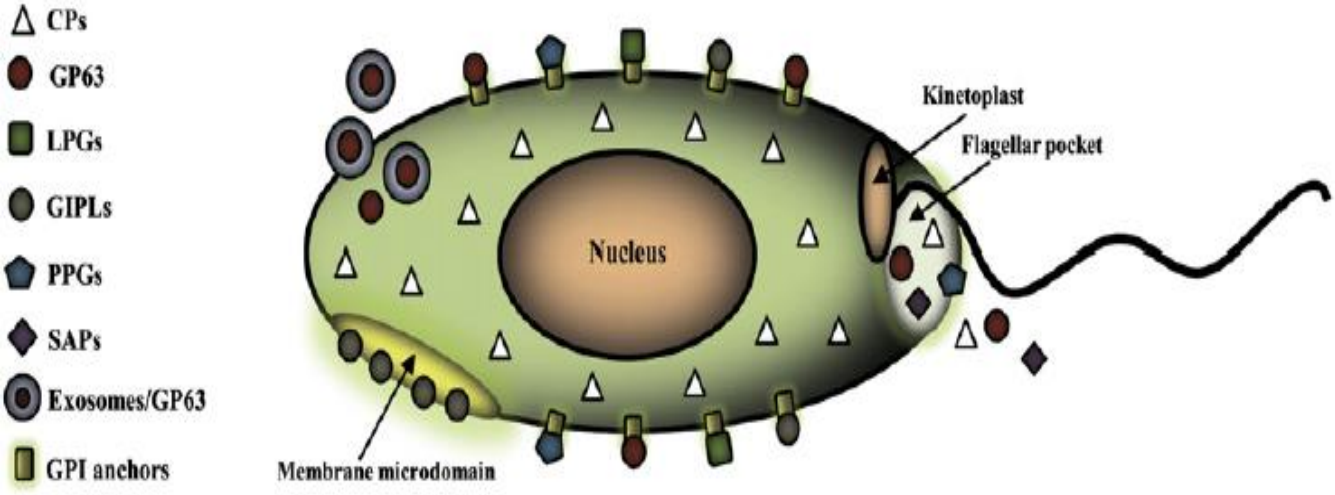

Figure 2: *Leishmania* virulence factors. A schematic representation of a promastigote showing cell surface glycoconjugates: LPGs, PPGs and GIPLs and virulence factors that are not membrane-anchored: GP63, PPGs, SAPs and CPs. Image taken from Olivier M, 2012 (33)**.**

3. Visceral leishmaniasis (VL)

Visceral leishmaniasis, also known as kala-azar, is caused by *L.infantum* in Europe, North Africa and Latin America or by *L.donovani* in East Africa and the Indian subcontinent. This infection represents the most severe form of leishmaniasis being fatal within two years if untreated. VL in adults is also considered an AIDS opportunistic disease and is characterized by a wide range of clinical symptoms caused by the parasite evasion into internal organs. There are two types of VL which differ in their transmission characteristics: (1) zoonotic, the natural mammalian reservoir are wild animals and domestic animals and human infection happens by overlapping habitats; (2) anthroponotic, the humans are considered the natural reservoir and occur in areas of *L. donovani* transmission (8,45). The epidemiological aspects are related to environmental changes and individual risk factors such as migration from urban to rural areas, movement of seasonal workers, large-scale migrations of population for occupational reasons, deterioration in social and economic conditions in the poor suburbs of cities, malnutrition and overlapping of VL and AIDS (8,9).

It is estimated that 500 000 new cases of VL occur yearly wherein 90% of them occur in Bangladesh, Brazil, Ethiopia, India, Nepal and Sudan. These infections are fatal in approximately 50.000 of the cases, being this death rate only surpassed by malaria (46). In the Old World (Africa, Asia and Europe), children are the most affected by endemic VL caused by *L. infantum.* However VL cases are rising among adults, mainly as an opportunistic co-infection in immunocompromised patients. This problem is particularly evident in Mediterranean countries such France, Spain, Italy and Portugal where half the cases are reported as coinfections, being the phenomena partly due to the extension of vector habitat in consequence of climate changes.

In Portugal, as in other countries in southern Europe, VL was initially pediatric. However, it has been observed a decrease in cases affecting children and an increase in adult HIV patients. Between years 2000 to 2009, the Leishmaniasis Unit of the Institute of Hygiene and Tropical Medicine, diagnosed 173 new cases of human VL: 66 in adults and in immunocompromised children and 107 in immunocompromised adults. In Portugal, the main foci of this infection are in the region of High Douro, Mondego river valley and the metropolitan area of Lisbon (47).

To contain the impact of this disease, control strategies are necessary and, currently this process involves control of reservoir and vector, early diagnosis, anti-leishmanial pharmacological treatment and the development of vaccines (8,45).

3.1 Clinical manifestations and Diagnosis

Visceral leishmaniasis is characterized by a wide range of clinical manifestations and can even be asymptomatic or subclinical in some cases. Following an incubation period that generally lasts between 2 and 6 months, VL patients present symptoms and signs of persistent systemic infection, including: fever, fatigue, weakness, diarrhea, loss of appetite and weight loss. In addition, VL causes hyperplasia of the visceral organs such as the spleen and liver (splenomegaly and hepatomegaly, respectively). A concomitant decreases in erythrocytes and leukocytes production results in anemia and granulocytopenia, facilitating secondary bacterial infection, especially pneumonia, dysentery and tuberculosis, the leading causes of death of VL patients. In a more advanced stage of the disease, the prothrombin production decreases and, together with

thrombocytopenia, may result in severe mucosal hemorrhage. The observed hypoalbuminaemia is associated with edema and other features of malnutrition (8,10,14,48). In the endemic areas of *L. donovani*, mainly in Sudan and less often in East African countries and in Indian subcontinents, after 6 months to 1 or more years of the treatment for VL, a complication called post-kala-azar dermal leishmaniasis (PKDL) may occurs. PKDL is characterized by a macular, maculo-papular or nodular rash and is highly infectious because the nodular lesions contain many parasites, representing this condition an important reservoir for anthroponotic VL (8,45).

In the treatment of human patients, an early diagnosis is essential because the signs and symptoms described above are not specific enough to differentiate VL from chronic malaria or other systemic infections. Thus, a laboratorial diagnosis is necessary to confirm the suspected VL. The detection of VL is done by parasitological diagnosis, serological diagnosis and antigen-detection tests (8,45,48). The parasitological diagnosis is the simplest, however not the more sensitive test, being based on the microscopic observation of the promastigote form of the parasite. The samples used in this procedure are extracted from tissue aspirate of the spleen or the bone marrow (49). The parasite identification can also be done by the detection of his DNA in blood or bone marrow aspirates by PCR. This procedure is more sensitive than the microscopic examination and can detect the parasite in asymptomatic patients however, PCR is only used in referral hospitals and research centers (8,48). The serological diagnosis involves techniques such as indirect fluorescence antibody technique (IFAT), enzyme-linked immunosorbent assay (ELISA), Western blotting (WB), direct agglutination test (DAT) and rK39-based immunochromatographic test (ICT). All of these methods provide good and accurate results however IFAT, ELISA and WB are not adequate for the field precarious conditions (8,50). On the other hand, DAT and ICT are particularly adequate for field use and represent easy and quick tests with low cost and reproducible results (8,51,52). Serological diagnosis have however two limitations: post-recovery cases are indistinguishable from active cases since specific antibodies remain detectable until years after the cure of the infection and a significant portion of healthy population in endemic areas exhibits anti-leishmanial antibodies but don’t have any history of VL (8,14,49). Accordingly, the serological tests must always be used together with a standardized clinical case definition for VL diagnosis (8). The antigen-detection tests are more sensitive than serological tests given they allow the

distinction of post-recovery cases from active cases and avoid cross-reactivity. A latex agglutination test to detect a heart-stable, low-relative molecular-mass carbohydrate antigen is a good option because this format is more adequate for application in rural areas where VL is endemic. The latex agglutination test is simple to use and it does not need any electric appliance and has a low cost (8,49).

3.2 Treatment

The treatment of VL requires complete bed rest and blood transfusions may also be necessary in some cases. Furthermore, chemotherapy is required and is the only treatment currently available for VL leishmaniasis (8,14). For more than half century, pentavalent antimonials have been used as first–line pharmacological approaches for VL treatment, however, currently these compounds has been replaced by amphotericin B and miltefosine. Pentavalent antimonials include chemicals such as sodium stibogluconate or meglumine antimonite (8,48,53). These compounds have a high efficacy, however they presents a wide range of toxic side effects, including: anorexia, vomiting, abdominal pain, myalgia, headache, lethargy, arthralgia, metallic taste, electrocardiographic changes, leukopenia, anemia, and thrombopenia. Uncommon, yet very serious side effects such as cardiotoxicity causing sudden death and pancreatitis have been also reported (8). Furthermore, the treatment with pentavelent antimonials is painful, invasive since it is done via intramuscular or intravenous routes, extensive (weeks to months), and the population of India and Nepal have developed resistance to these drugs (46). Other drugs intravenously administrated for the VL treatment are amphotericin B, its lipid formulations and pentamidine, which are used in countries where the population is resistant to pentavalent antimonials (48). More recently, with the discovery of miltefosine's antileishmanial properties, oral treatment became available allowing a less invasive mode of administration, however this drug is teratogenic and expensive (8,45,48). Actually, a human anti-leishmanial vaccine is not available despite the intense investigation focused in this issue. The attempt for the discovery of an efficient immunizing therapy has been difficult due to the variety of the parasites involved in leishmnaniasis. However, after the recovery from the infection the immunity against the parasite is strong, thereby indicating that the development of a vaccine for humans would represent the ultimate therapeutic approach (8,45).

4. Host-pathogen interaction: *Leishmania*-macrophage

The outcome of *Leishmania* infections strongly depends on the *Leishmania* specie involved and on the immune status of the host. When the host immune system is compromised as in HIV patients, the infection is facilitated. It is therefore crucial the knowledge about the interactions of parasites with immune cells, particularly whit macrophages due their role in the control of the disease (8).

The immune response consists of two complementary arms: the humoral and cellular immune systems. In the control of *Leishmania* infections, cellular immune system plays a crucial role. Macrophages are cells with high phagocytic activity and moderate antigen-presenting abilities. These cells represent mature monocytes cells and are the primary effectors for *Leishmania* elimination, having a variety of strategies to prevent the survival of infecting parasites. The major pathogen-killing mechanisms of macrophages results from an oxidative burst due to the production of reactive nitrogen and oxygen species, such as superoxide (O_2^-), hydrogen peroxide (H_2O_2), and hydroxyl ions ($-OH^-$), leading to the parasite degradation. The parasite internalization is facilitated by complement receptor-mediated recognition of surface-bound C3b and/or C3bi opsonins (1,54,55). Macrophages produce many digestive enzymes, bactericidal agents and also interact with T helper cells (Th1 or Th2 cells), whose function is to produce cytokines like TNF-α, Interleukine-6, IL-8, IFN-γ and IL-12 (54,55). Another important molecule produced by macrophages is nitric oxide (NO), which is known to have an important role in the immune system and inflammation (56). However, even with the deleterious mechanisms described above, *Leishmania* parasites establish a complex interaction with macrophages, avoiding their lytic mechanisms and subverting their immunostimulatory functions (6).

4.1 Macrophages proteins altered by *Leishmania*

To enter in host cells, metacyclic promastigote take advantage of opsonization with C3 and C3bi, which bind to the macrophage receptors CR1 and CR3, respectively. Adopting these receptors for entry, *Leishmania* avoid the oxidative burst since CR1 and CR3 don't promote this process (57). Furthermore, CR3 inhibits the IL-12 induced cell-mediated immunity, protecting promastigotes from deleterious effects of effector T cells (57,58). Additionally to the receptors CR1 and CR3, the receptor CR4, mannose-fucose

receptor, FcγRI, FcγRII, C-reactive protein receptor and the receptor for advanced glycosylation end products (RAGEr) were shown to be involved in parasitic adhesion and phagocytosis (59–61). Once in the host, and in order to survive, *Leishmania* parasites actively impair several host signaling effector molecules such as cellular kinases, cellular phosphatases, transcription factors and cytokine production among others (Figure 3).

One of the kinases affected by *Leishmania* is Janus kinase 2 (JAK 2), a member of the Janus family of tyrosine kinases that play an important role in immune activation. The JAK signaling pathway starts when a cytokine or a growth factor binds to its receptor inducing a signaling cascade that ultimately results in the phosphorylation of a signal transducer, an activator transcription (STAT) and a transcription factor (TF) that consequently leading to the activation or repression of gene transcription (62). The alteration of the JAK signaling is advantageous for the *Leishmania* because the iNOS gene promoter has binding sites for several TFs and the parasite has the ability to block the JAK/STAT signaling pathway in response to the IFN-γ stimulation, thus decreasing NO production by macrophages (63). Nandan and Reiner reported that infection with *L. donovani* amastigotes was able to block IFN-γ-induced JAK1, JAK2, and STAT-1 phosphorylation in PMA differentiated U-937 promonocytic cells and human monocytes (64). Another study demonstrated that *L. donovani* promastigotes rapidly activate host SHP-1 leading to the subsequent inhibition of IFN-γ-induced JAK2 phosphorylation (65). The mitogen-activated protein (MAP) kinases family also seems to be modulated by *Leishmania* parasites. The MAP kinases are serine/threonine kinases that link transmembrane signaling with gene transcription events and are divided in three major subgroups: the extracellular signal-regulated kinases (ERKs); the p38 MAP kinase and the c-jun amino-terminal kinases (JNKs). It has been reported that synthetic *Leishmania* LPGs activate ERK MAP kinase in macrophages which suppress the transcription of IL-12p40 (66). Another kinase affected by the parasite is protein kinase C, which activity was shown to be decreased by *Leishmania* LPG (67).

Protein tyrosine phosphatases (PTPs) are proteins that have the ability to remove the phosphate from P –Tyr residues, reversing the effect of phosphorylation (55). Included in these PTPs are PTB-1, TC-PTP and SHP-1, which play an important role in *Leishmania* ability to evade host immune system evasion mechanisms (68). PTB-1 is related to the regulation of cytokine signaling through its interaction with JAK-2 and TYK2 and its

ability to dephosphorylate these kinases. As mentioned in the section 1.1.2, PTPs are modulated by *Leishmania* GP63. Activation of the protein tyrosine phosphatase TC-PTP represents an advantage to the parasite since it plays an important role in the negative regulation of JAK1, JAK3 and nuclear STAT-1 (69,70). The PTP SHP-1 is recognized as a negative regulator of several phosphotyrosine-dependent signaling cascades involved in the immune response, thus it is also important in *Leishmania* parasite survival. It has been reported that macrophages defective in SHP-1 are more efficient in limiting *Leishmania* survival and SHP-1- deficient mice display a decreased inflammation during *L. donovani* infection an observation that is associated with increased NO production (71).

Another target during *Leishmania* infection is the transcription factor NF-κB. The NF-κB family of transcription factors consists of five different members containing Rel homology domain that play crucial roles in the innate immune responses by regulating the expression of many pro-inflammatory mediators such as chemokines and cytokines, among others (72). It has been reported that mice deficient in a variety of NF-κB family members were susceptible to many viral, bacterial and parasitic evasion, revealing the importance of NF-κB in protection against infections (72). Guizani-Tabbane and collaborators showed that *L. major* amastigotes induce p50/cRel NF-κB complexes, leading to TNF-κ and IL-10 expression (73).

As mentioned before, under parasitic interaction, the macrophage produces a wide range of cytokines such as IL-1, IL-18, IL-12, tumor necrosis factor (TNF)-α, among others. These molecules are responsible for a variety of biological effects in the immune system and can be divided in two groups: the proinflammatory (e.g., IL-1, IL-12 and IFN-γ) and anti-inflammatory (e.g., IL-4, IL-5, IL-10 and IL-13) cytokines. Cytokines are mainly produced by T helper cells, being Th1 and Th2 cells connoted with production of proinflammatory or anti-inflammatory cytokines, respectively. Thus, the balance between Th1 and Th2 responses is crucial to a proper response of the immune system to an infection (55,74). *Leishmania* parasites alter this balance, favoring a Th2 response, namely through the production of IL-4, IL-5, IL-10 and IL-13 and inhibiting Th1 response by decreasing the level of pro-inflammatory cytokines IL-1, IL-12 and IFN-γ levels. It has been reported that infection of BMDMs with promastigotes of *L. major* or *L. donovani* fails to induce IL-12 production, both following infection alone and upon subsequent LPS or heat-killed bacterial macrophage stimulation (75). Another study reported that IL-1 and

TNF-α are not produced upon a 12h *in vitro* infection of human monocytes with *L.donovani* amastigotes (76).

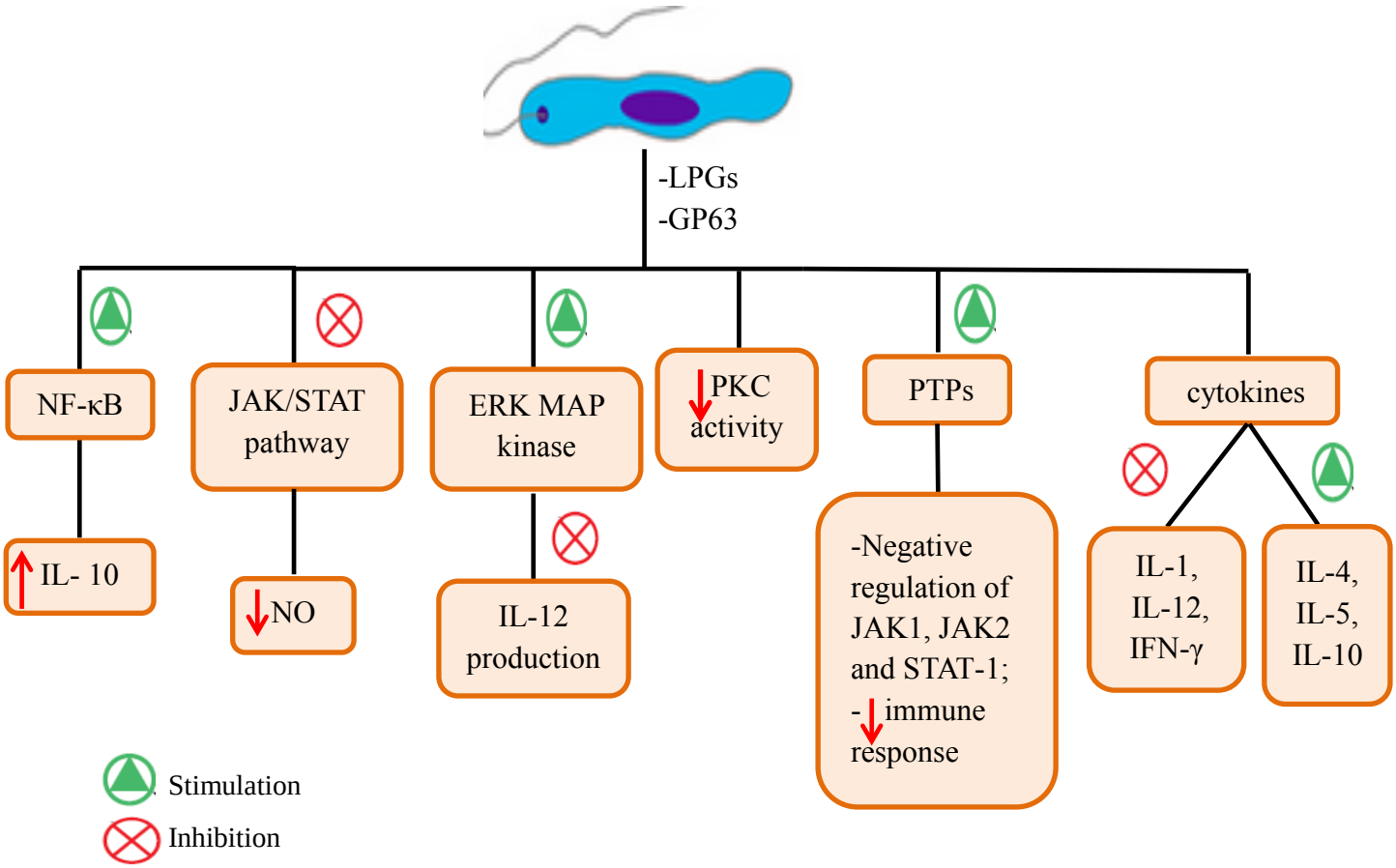

Figure 3: Schematic representation of some mechanisms used by *Leishmania* parasites to evade/subvert macrophage immune functions.

4.2 Macrophages lipids altered by *Leishmania*

As mentioned in the previous section, macrophage protein alterations by *Leishmania* parasites are numerous and extensively studied. Regarding the modifications of the macrophage's lipids profile by *Leishmania*, little is known. However due to the growing body of data about the immunomodulator functions of lipids they can be a promising therapeutic target for the treatment of the infection. Changes in lipid homeostasis of *Leishmania*-infected macrophages were already reported, namely the depletion of macrophage cholesterol induced by L. major, with consequences on the signals transmitted by CD40 engagement (77). CD40 is a co-stimulatory molecule which binds CD40 ligand (CD40L) and signals trough p38 and ERK1/2 mitogen activated protein kinases to regulate IL-12 and IL-10, respectively. In uninfected macrophages, strong CD40

stimulation induces the activation of p38 MAPK, thus the expression of IL-12, whereas weak CD40 stimulation triggers the activation of ERK1/2 signaling cascade and the consequent production of IL-10. In macrophages infected with *L. major*, the production of anti-inflammatory cytokine IL-10 is enhanced, probably as the results of modulation of the CD40 signaling by parasites (77). A mechanism proposed to the alteration of CD40 signal transduction is the depletion of the macrophages membrane cholesterol caused by the parasite. This hypothesis results from the observation that CD40 signaling is inhibited by β-methyl-cyclodextrin (β-MCD)-mediated depletion of membrane cholesterol (77,78). It has been reported that in *L. major*-infected macrophages, CD40 signaling is mediated by distinct signalosomes, depending on the location of CD40 in cholesterol-depleted or cholesterol-repleted membrane fractions. The presence of CD40 in cholesterol-depleted favors the phosphorylation of ERK1/2 whereas the location of CD40 in cholesterol-depleted favors the phosphorylation of p38 MAPK. It has also been reported that mevalonate, a cholesterol precursor, enhanced the CD40-induced phosphorylation of Lyn and p38 MAPK but inhibited the CD40-induced phosphorylation of Syk and Erk1/2, increasing the CD40-induced anti-leishmanial function in *L. major*-infected macrophages (77). However the effect of parasites on cholesterol metabolism is controversial given that other studies reported that *L. major* parasite induces cholesterol accumulation and foam cell formation (79).

Sphingolipids (SLs) in macrophages are also targets of *Leishmania* parasites during the infection (80). SLs consist in important components of the membrane and their metabolites such as ceramide (CER), an unmodified sphingolipid, and sphingosine-1-phosphate control multiple processes, including cell growth, differentiation and apoptosis (81). Mammals require the sphingolipid synthase, SM synthase (SMS), for the biosynthesis of its most abundant sphingolipid, sphingomyelin (SM). This reaction occurs via the transfer of phosphorylcholine from phosphatidylcholine (PC) to CER to give SM. On the other hand, *Leishmania* parasites don't synthetize SM, but rather use IPC synthase to catalyze the inositol phosphorylceramide (IPC), via the transfer of phosphorylinositol form phosphatidylinositol (PI) to CER (80,82,83). It has been reported that intramacrophage amastigotes synthesize the complex sphingolipid IPC *de novo* using precursors from the host and maintain this lipid species at equivalent cellular levels to promastigotes (80). Another study demonstrated that *L. donovani* stimulate host macrophages to up-regulate

the production of CER, a substrate for IPC synthase (84). Furthermore, a recent work has identified the *L. major* sphingomyelinases (*Lmj*ISCL), an enzyme that degrades SM, and showed it to be essential for pathogenicity in an animal model (85). The studies referred above suggest that de SLs of the host are used and essential for the infectivity and survival of *Leishmania* parasites inside macrophages. It has also been suggested that CER play a role in *Leishmania* infectivity. CER act as second messenger and participates in cell growth, differentiation, immunomodulation, apoptosis and induced inflammatory response. Gosh and collaborators demonstrated that a significant elevation of intracellular CER occurred in *L. donovani* infected macrophages (84). Furthermore, this study revealed that elevation of intracellular CER was associated with down regulation of classical calcium dependent PKC, enhanced expression of atypical PKC-ζ isoform, decreased MAPK activity and NO generation. These findings suggested that ceramide helps parasite uptake and survival, being responsible for the down regulation of several important intracellular signaling cascades in infected cells (86).

4.3 Other host-pathogen interactions: a lipidic point of view

Besides the above referred studies, data regarding the effects of *Leishmania* parasites on the macrophage lipidic profile and their functional consequences remains very scarce. However, they are several studies reporting lipid alterations in the host cell induced by other microorganisms such as: dengue virus (DENV) and hepatitis C virus (HCV).

The dengue virus (DENV) is spread by *Aedes aegyptii* and *Aedes albopictus* mosquitoes and is responsible for the dengue fever. For the transmission from the mosquito to the human host occur, the viral replication within the vector is required. This process causes significant alterations into the membrane organization of the infected mosquito cells in order to help the virus replication and assembly. A global lipidome study of mosquito cells infected by DENV, using high-resolution mass spectrometry, demonstrated a selective enrichment of lipids involved in membranes structure as well as those that have potent signaling functions (87). Identified molecules include bioactive sphingolipids such as SM and CER, lysophospholipids (LPLs) and several intermediates such as mono- and diacylglycerol (DAG) and phosphatidic acid (PA). This work also showed an up regulation of *de novo* phospholipid and sphingolipid biosynthesis and that unsaturated PC is strongly

up regulated in DENV infected cells (87). It was shown that in the presence of C75, an inhibitor of the rate limiting enzyme fatty acid synthase (FAS), DENV replication is significantly reduced in C6/36 mosquito cells, indicating that fatty acid biosynthesis is important for virus viability. Furthermore, a time course experiment revealed that pre-treatment or treatment of cells with C75 during viral adsorption reduced virus replication by 10 to 100 fold being the most significant effect upon addition of the drug at 4 and 8 hours post-infection (1000 fold). This observation strongly suggests that a post-entry step was affected by the inhibition of FAS (87).

Another pathogen that was shown to alter host cell lipid homeostasis is the Hepatitis C virus (HCV). HCV integrates the *Flaviviridae* family and consists in a major cause of liver disease, being a global public health problem. It has been suggested that HVC alters the lipid metabolism of the host cells and that this process is crucial for the virus life cycle (88). A lipidome analysis during infection of Huh-7.5 (human hepatoma cell line) with HCV demonstrated a progressive accumulation of several phosphatidylcholine and phosphatidylethanolamine species of the host cell at 48 and 72 hours post-infection relative to either the mock or UV-inactivated HCV samples. In contrast to the accumulation of these lipid species, it was observed a progressive decline of cholesterol esters, triacylglycerols, SMs, PC 35:1 and phophatidylethanolamine 38:3 during the accumulation of extracellular infectious virions. This data suggests that these lipids are probably consumed during HVC assembly and secretion. The decline of some SMs may also result be the consequence of their utilization for the synthesis of reactive CER which are shown to be increased (88).

Although scarce, data regarding host cell lipid homeostasis modification by pathogens indicate that these processes could have crucial roles in installment and progression of infections. Few reports approach *Leishmania* parasites interference with macrophages, lipid profile and their biological consequences. Therefore, new studies focused on the host-pathogen interactions at the lipidic level are required in order to identify novel therapeutic targets for the treatment of this infection.

5. Lipids: structure and biological functions

Lipids are essential constituents of the cell that play important roles in cellular functions, including: (1) the production of second messengers (e.g., araquidonic acid and diacylglycerol) trough enzyme reactions; (2) the capacity to delimit the cell, making it relatively independent of the exterior environment due to the lipid bilayer structures, (3) the capacity to provide the cell an appropriate hydrophobic environment for an adequate functionality and interactions of proteins and (4) they represent an easy and quick energetic storage to access. Lipids consist in a huge number of structurally and functionally distinct molecular species and their defining and common feature is their insolubility in water. Lipids can be apolar (e.g., sterol esters), neutral (e.g., triacyglycerides) and polar (e.g., phospholipids) (55,89). Fatty acids (FAs) represent the simplest and one of the most important lipid classes. Structurally, FAs are carboxylic acids with saturated or unsaturated hydrocarbon chains ranging from 4 to 36 carbons long (C4 to C36). FAs are precursors of a variety of bioactive lipid molecules. An example of a molecule modulate by FAs is the arachidonic acid being the precursor of eicosanoids, which function as signaling molecules through specific receptors and play important roles in inflammatory processes (55,89).

Most of cellular lipids form membrane bilayers are composed mainly by phospholipids, which are fundamental in biological systems and cell to cell communication processes. Membranes define the external boundaries of cells, regulate the molecular traffic across that boundary and its fluidity control, at least in part, the ligand-receptor interaction, endocytosis and antigen presentation (55,90). Biological membranes are flexible, self-sealing and selectively permeable to polar solutes. These specific properties of membranes are due to their constituents, namely the PLs, and their arrangement in bilayer in which the nonpolar regions of the lipid molecules in each layer face the core of the bilayer and their polar head groups face outward, interacting with the aqueous phase on either side. The lipids and the proteins of the cellular membrane form a fluid mosaic since most of the components interactions are noncovalent, being free to change constantly (55). PLs, the mainly constituents of cellular membranes, are amphipathic molecules having a head constituted by a phosphate group linked to other specific group, depending on the class of lipid, which is polar or hydrophilic and a tail consisting of the FA chains that are nonpolar or hydrophobic, both linked by a glycerol molecule. These amphipathic molecules allows the organize structure observe in cellular membranes.

PLs are also called glycerophospholipids (GLs) and are membrane lipids in which two FAs are attached in ester linkage to the first and second carbons of glycerol, and a highly polar or charged group is attached through a phosphodiester linkage to the third carbon. GLs are named as derivatives of phosphatidic acid, according to the polar alcohol in the head group. Within the GLs are: phosphatidic acid (PA), phosphatidylethanolamine (PE), phosphatidylcholine (PC), phosphatidylserine (PS) and cardiolipin (CL) among others, differing in their polar alcohol in the head group (Figure 4). These lipids are key components of cellular membranes, serve as binding sites for cellular and extracellular proteins and their metabolites act as second messengers, being involved in proliferation and apoptotic cell injury (55,81).

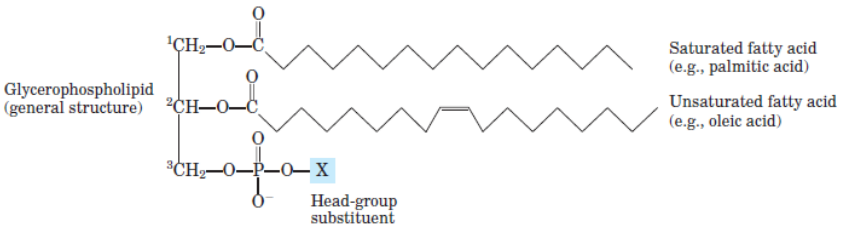

Glycerophospholipid	Name of x	Formula of x
Phosphatidic acid (PA)	-----	— H
Phosphatidylethanolamine (PE)	Ethanolamine	— CH_2—CH_2—$\overset{+}{N}H_3$
Phosphatidylcholine (PC)	Choline	— CH_2—CH_2—$\overset{+}{N}(CH_3)_3$
Phosphatidylserine (PS)	Serine	— CH_2—CH(—$\overset{+}{N}H_3$)—COO^-
Phosphatidylglycerol (PG)	Glycerol	— CH_2—CH(—OH)—CH_2—OH
Phosphatidylinositol 4,5-bisphosphate	*myo*-Inositol 4,5 bisphosphate	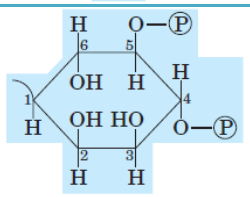
Cardiolipin	Phosphatidyl-glycerol	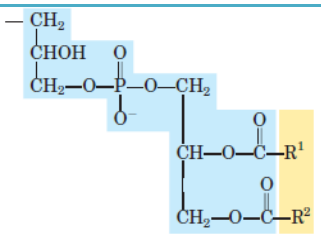

Figure 4: Molecular structure of the different GLs. Adapted from Lehninger Principles of Biochemistry (55).

Sphingolipids (SLs) are composed of one molecule of the long-chain amino alcohol sphingosine or one of its derivatives, one molecule of a long-chain fatty acid, and a polar head group that is joined by a glycosidic linkage in some cases and by a phosphodiester in others however, unlike GLs they contain no glycerol. Belonging to this class of lipids are:

ceramide (CER), sphingomyelin (SM), neutral glycolipids, among others (Figure 5). SLs are involved in signal transduction and cell recognition (55,81). The SM together with cholesterol form lipid rafts: the cholesterol fills the spaces along the SM molecules resulting in membrane domains enriched in SM and cholesterol. These domains play an important role in the cell signalization since some protein components of signaling transduction pathways have a great affinity for these lipid rafts (91).

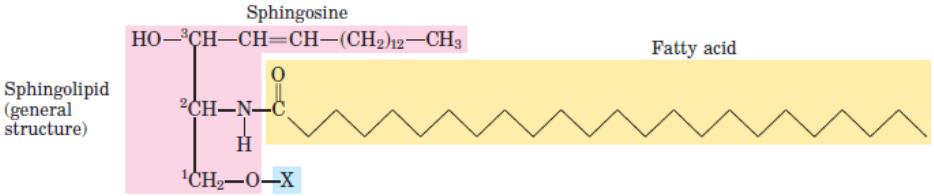

Sphingolipid	Name of x	Formula of x
Ceramide	-----	— H
Sphingomyelin	Phosphocholine	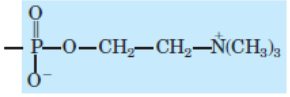
Neutral Glycolipids Glucosylcerebroside	Glucose	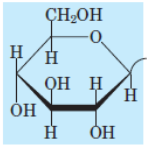
Lactosylceramide (a globoside)	Di,tri or tetrassacharide	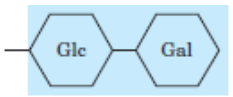
Ganglioside GM2	Complex oligossacharide	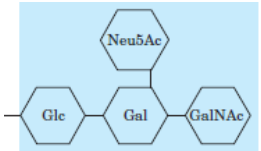

Figure 5: Molecular structure of the different SLs. Adapted from Lehninger Principles of Biochemistry (55).

Other lipids are also present in cells and although being present in smallest quantities, they play important roles such as: enzyme cofactors, electron carriers, hydrophobic anchors for proteins, emulsifying agents in the digestive tract, hormones, and intracellular messengers. For example, the eicosanoids are hormones derivatives of

araquidonic acid and are involved in several biological processes including: in the reproductive function; in the inflammation, fever and pain associated whit injury or disease; in blood clots, among others (55).

As mentioned above, lipids are structurally and functionally diversified, being involved in interaction with proteins thereby participating in several signaling pathways essential to adequate cell functioning. Thus, the identification of lipid profiling or their change is important to understand the living being homeostasis or disease and it requires complementary approaches casually called lipidomics.

6. Lipid analysis: a lipidomic approach

Lipidomics consists in "the large-scale analysis of lipids in cells and tissues" (92). Lipidomic can be understood as a specialized field of metabolomics, which covers the study of metabolic profiles through the analysis of metabolites such as lipids and proteins (93). Lipidomics area extensively analyzes the different lipid classes, both qualitatively and quantitatively, their interaction with other molecules, their role in cellular signaling pathways and the changes they suffer in a pathological situation (94). Thus, there are two focal points that lipidomic pretends to elucidate: how to link lipid metabolites and/or lipid metabolic pathways in complex biological systems to individual metabolic health and how to interpret the changes in the lipid metabolism or in the regulation of these pathways linked to metabolic and inflammatory diseases from a physiological and/or pathological perspectives (89).

Lipids were target of intense research in the 60's due to their importance in biological processes; however the analytical techniques available at the time were limited compare to the techniques for molecular biology, genomics and proteomics (95). Furthermore, lipids are highly diversified and complex, therefore measuring all types of lipids within a total lipid extract is a challenge (93). The advent of modern techniques such as: nuclear magnetic resonance (NMR), fluorescence spectroscopy, chromatography in column and mass spectrometry (MS) made lipidomics gain an increased importance and interest over the years. Mass spectrometry has been successfully coupled to front-end separation or used directly (shotgun lipidomics) to allow the identification of specific molecular lipids together with their quantification. This technique was one of the main

contributors to the growth of lipidomics (81,90). The strategies underlying the lipidomic approaches involve several procedures such as: (1) the isolation of membranes morphologically distinct or sub fractions from tissues or cells by specific methods that take advantage of the high solubility of the hydrocarbon chains of lipids in organic solvents; (2) the extraction of lipids from membrane proteins and other components, (3) after extraction, lipids are separate through chromatography procedures. These procedures allow the identification and quantification of each lipid by MS thereby creating a lipid profile (Figure 6). Regarding the phospholipids, the most common extraction methods are the Bligh and Dyer and Folch methods and, after the separation of the PLs classes by chromatographic methods, the PLs content of each class can be measured by phosphorous assay that measures the inorganic phosphate present in the sample (81,96,97).

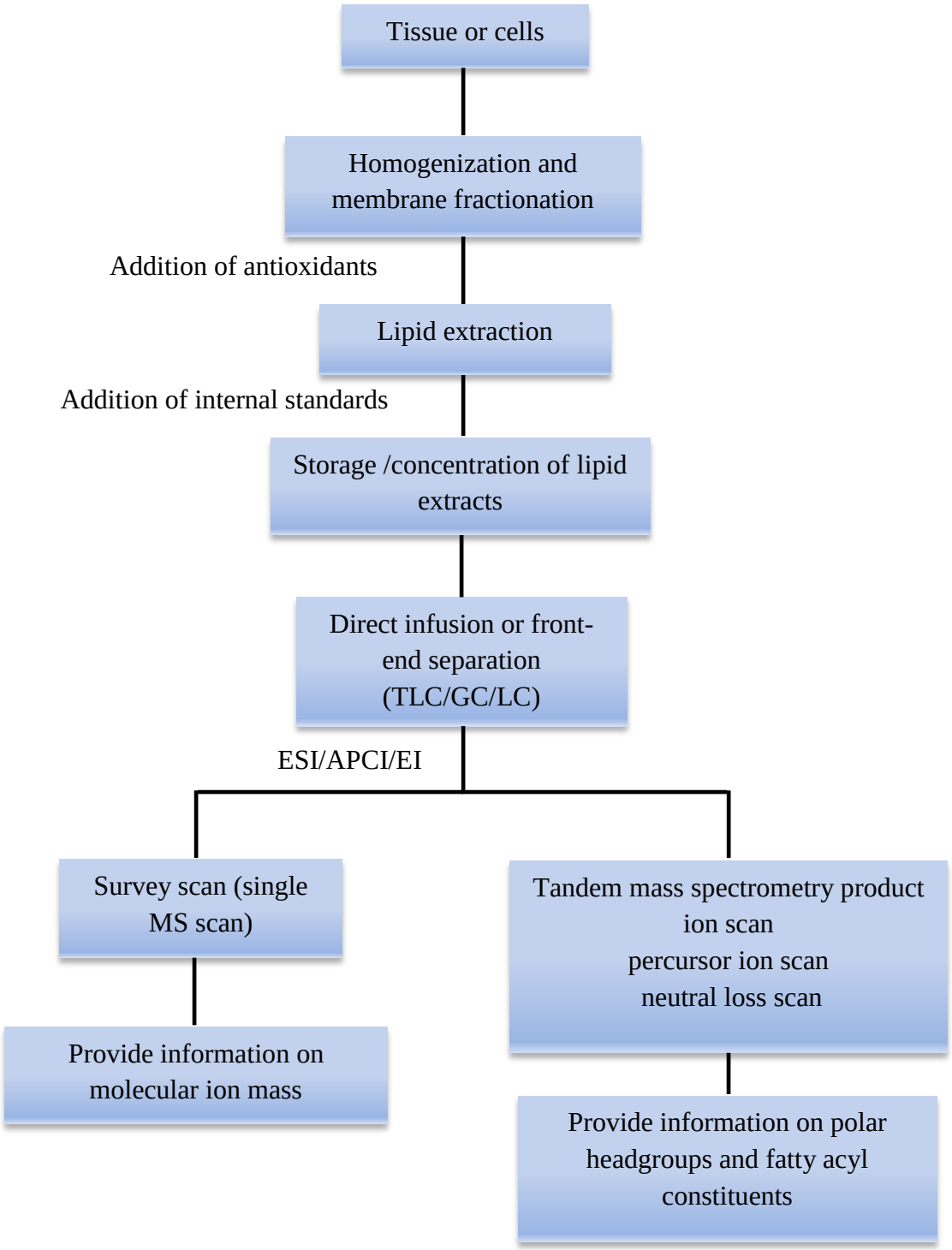

Figure 6: A schematic diagram of the overall lipidomic approache. Adapted from Lipidomics era: accomplishments and challenges (81).

Lipidomics is now considered an integral part of system biology, being an active topic of interest. This field has been enabled great breakthroughs since it related lipids imbalances to several diseases. For example, imbalances in lipid homeostasis are associated with Alzheimer's, Parkinson's, Niemann-Pick, multiple sclerosis, Huntington, amyotrophic lateral sclerosis, schizophrenia, bipolar disorders, epilepsy and central nervous system injury. Thus, lipidomics provide important insights about the stage of a disease and the cell homeostasis since the alterations at lipid level can elucidate alterations in genes and proteins and vice-versa. Lipidomics together with genomics, proteomics and metabolomics will provide a powerful tool to a better understanding of molecular mechanisms related to lipid-associated disorders, and to identify biomarkers and novel therapeutic targets (81).

7. Aims

Leishmaniasis is still one of the world's most neglected diseases, affecting in developing countries a significant number of people. *Leishmania* parasites established complex interactions with immune cells such as macrophages and dendritic cells, disrupting their normal functioning in order to survive. In the last decades, innumerous works have shown that these mechanisms resulted from modifications caused by parasites in key cellular proteins. Regarding the effects of *Leishmania* in host cells lipid profile, little is known. However, due the growing knowledge of lipid immunomodulatory functions, they can be viewed as a promising therapeutic target for the treatment of this infection.

Therefore, the general aim of this work is to analyze the variation in lipidomic profile of *L. infantum*-infected mouse macrophages in order to elucidate the contribution of lipidic changes to the pathogenesis of this infection. Lipid profile of infected macrophages will be evaluated and compared with non-infected (control) and with macrophages infected with killed parasites, using a lipidomic approach. After this, key proteins/enzymes involved in metabolic pathways related to the observed lipid alterations will be evaluated.

II. Material and Methods

III. Material and Methods

1. Materials

The phosphatidylethanolamine (PE), phosphatidylserine (PS),phosphatidylcholine (PC), phosphatidylinositol (PI), phosphatidic acid (PA), sphingomyelin (SM), phosphatidylglycerol (PG), lysophosphatdylcholine (LPC), lysophosphatidylinositol (LPI), phosphatidylethanolamine (LPE), lysophosphatidic acid (LPA) and cardiolipin (CL) standards were purchased from Sigma-Aldrich (Madrid, Spain), triethylamine (Acros Organics), chloroform (HPLC grades), methanol (HPLC grades), ethanol (Panreac), primuline (Sigma) were used without further purification. TLC silica gel 60 plates with concentration zone (2.5x20cm) were purchased from Merck (Darmstadt, Germany).

Penicillin, streptomycin, Roswell Park Memorial Institute (RPMI) 1640 and Dulbecco's Modified Eagle Medium (DMEM) mediums were obtained from Sigma Chemical Co. (St. Louis, MO, USA). Fetal Bovine Serum and TRIzol reagent were from Invitrogen (Paisley, UK). The protease and phosphatase inhibitor cocktails were obtained from Roche (Mannheim, Germany). The anti-tubulin antibody was purchased from Sigma Chemical Co. (St. Louis, Mo, USA), anti-COX2 antibody from Santa Cruz Biotechnology (Heidelberg, Germany)and anti-COX-1 from Abcam (Cambridge,UK). The alkaline phosphatase-linked secondary antibodies and the enhanced chemifluorescence (ECF) reagent were obtained from GE Healthcare (Chalfont St. Giles, UK), and the polyvinylidene difluoride (PVDF) membranes were from Millipore Corporation (Bedford, MA). iScript kit and SYBR green were obtained from BioRad (Hercules, CA, USA). Primers were from MWG Biotech (Ebersberg, Germany). The provenience of all other reagents is specified along the text.

2. Culture of Macrophages

Raw 264.7 (ATCC number: TIB-71), a mouse macrophage cell line kindly supplied by Dr. Otília Vieira (Center for Neuroscience and Cell Biology, University of Coimbra, Coimbra, Portugal) was cultured DMEM medium supplemented with 10% non-inactivated fetal bovine serum, 100 U/mL penicillin, and 100 μg/mL streptomycin at 37°C in a humified atmosphere of 95% air and 5% CO2.

3. Culture of Parasites

A cloned line of virulent *L. infantum* (MHOM/MA/67/ITMAP-263) was maintained by weakly subpassages (less than 10) in complete RPMI 1640 (RPMIc) supplemented with 10% heat-inactivated fetal bovine serum (FBS), 100 U/ml penicillin, 100 mg/ml streptomycin, and 2 mM HEPES (BioWhittaker).

4. Lipid Extraction

Total lipid extracts were obtained from the macrophages cell lines in the different conditions using the Bligh and Dyer method (98). HPLC solvents (chloroform and methanol) and milli-Q purified water were used during lipid extraction procedure. For 1 ml of sample in water, we added 3.75 ml chloroform /methanol 1:2 (v/v), vortexed well, and incubated on ice for 30 min. Then, an additional volume of 1.25 ml chloroform was added and finally 1.25 ml mili-Q H_2O. Following vigorous vortex, samples were centrifuged at 1000 rpm for 5 min at room temperature to obtain a two-phase system: aqueous top phase and organic bottom phase with chloroform from which lipids were obtained. The organic phase was separated into a new tube, dried in a nitrogen flow and ressuspended in 300 µl of chloroform making our extracts ready for the following analysis: TLC and LC-MS.

5. Phosphorous Assay

In order to quantify the total amount of PLs as well as amounts of each PL class in separated by TLC, a phosphorous assay was performed according to Bartlett and Lewis (99).To quantify the total PL extract, 10 µl the total lipid extract, after the Bligh and Dyer method was used, and dried with a nitrogen flow. To quantify the different classes separated by TLC, the spots were scraped off from the plates directly to the quantification tubes. Next, we added 6,5 ml of perchloric acid (70%) (Panreac) to samples which were then incubated in a heating block (Stuart) 45 min at 180°C. After cooling, 3.3 ml of mili-Q H_2O, 0.5 ml of 2.5% ammonium molybdate (Riedel – de Haën) and 0.5 ml of 10% ascorbic acid (VWR BDH Prolabo) were added to all samples, vortexing always after the addition of each solution. Then, the samples were incubated for 5 min at 100°C in a water bath. Standards from 0.1 to 2 µg of phosphorous (P), prepared from a phosphate standard solution of dihydrogenphosphate dihydrated ($NaH_2PO_4.2H_2O$) (Riedel – de Haën) with 100

μg/ml of P, underwent the same treatment as the samples. The absorbance of the samples, after cooling, was measured at 800 nm (Multiskan 90, Thermoscientific). In the case of TLC separated lipid classes, prior to spectrophotometric determination, samples were centrifuged 5 min at 4000 rpm to separate PLs from silica. The amount of phosphorus present in each sample was calculated by linear regression through the graph relating the amount of phosphorus present in the patterns (X-axis) with absorbance obtained from duplicates of various concentrations (Y-axis). The amount of phospholipid was calculated by multiplying the amount of result phosphorus by 25. The percentage of each PL class was calculated by relating the amount of PL in each TLC spot to the total amount of PL in the sample, thus giving the relative PL content (%) of each PL class.

6. Thin Layer Chromatography

PL classes from the total lipid extract were separated by thin layer chromatography (TLC) using silica gel plates with concentrating zone 2,5x20cm (Merck). Prior to separation, plates were washed in a methanol : chloroform mixture (1:1, v/v) and left in the safety hood for 20 min. Plates were then sprinkle with boric acid (2.3% m/v) (DHB chemicals) and dried in an oven at 100ºC during 30 min. 20 μl of phospholipid solution in chloroform (with a concentration of 150 μg of phospholipid per 100 μl) was applied in the plates. The plates were dried in a nitrogen flow and developed using the solvent mixture composed by chloroform, ethanol (Panreac), water and triethylamine (Merck) with a proportion of 30:35:7:35 (v/v/v/v). After the elution the plates were lefted in the safety hood until the eluent was completely dried. Lipid spots on TLC plates were observed after spraying a primuline solution of 50μg/100 ml (acetone : water 80:20, v/v), and visualized with a UV lamp (366 nm). The comparison of the spots observed with phospholipids standards (LPC, SM, PC, PI, PS, PE, PA, CL), run side by side in the TLC plate, allowed the identification of the different classes of PLs. Then, the spots were scraped off from the plates in order to quantify the amount of phosphorus using the phosphorous assay

7. Fatty Acid Quantification by Gas Chromatography with Flame Ionization Detector (GC-FID)

The fatty acids profile of lipid extract of macrophages in each condition was analyzed by GC-FID with the method proposed by Pimentel and colleagues (100). Briefly, it uses KOH in methanol trans-methylation in order to form fatty acid methyl esters (FAMEs). To perform the trans-methylation, we used 40 µg of total extracts that were transferred to centrifuge tubes and dried in nitrogen flow. Then, it was added 1 ml of methyl heptadecanoate (C17:0) internal standard solution (0.75g/L in n-hexane with 1:100 dilution). After the addition of internal standard, 0.200 ml of KOH (2M) in methanol were added, and the mixture was vortexed well (1-2 minutes). The mixture was then centrifuged at 2000 rpm during 5 minutes. The upper phase was collected into eppendorfs and the solvent was dried in nitrogen flow. Finally, the sample was ressuspended in 20 µl of n-hexane, and 4 µl of this solution were injected to the chromatograph. Fatty acids were identified by the retention times previously determined with the same procedure with a mixture of standard fatty acids. The peak areas of the fatty acids were used to calculate their relative amount. Data acquisition and analysis was done using TotalChrom Navigator Software.

The GC injection port was programmed at 250ºC and the detector at 270ºC. Oven temperature was programmed in three ramps, 50ºC for 3 min, 25ºC/min until 180ºC for 6 min and 40ºC/min until 260ºC for 3 min performing 19 min totally. The carrier gas was hydrogen flowing at 1.7 ml/min. The column used was DB1 with 30 m, internal diameter of 0.250mm and 0.10 µm film thickness.

8. High-Performance Liquid Chromatography (HPLC)

In order to identify the molecular species and their changes in macrophages exposed to *Leishmania-infantum* promastigotes phospholipid classes were separated by LC-MS, using a HPLC system (Waters Alliance 2690) coupled to an electrospray (ESI) linear ion trap mass spectrometer(ThermoFinnigan, San Jose, CA, USA). The mobile phase A consisted of 10% water and 55% acetonitrile with 35% (v/v) of methanol. The mobile phase B consisted of acetonitrile 60%, methanol 40% with 10mM ammonium acetate. 15 µl of total lipid extract were diluted in the mobile phase A and reaction mixture

was introduced into a Ascentis Si HPLC Pore column (15 cm×1.0 mm, 3 μm) (Sigma-Aldrich). The solvent gradient was programmed as follows: gradient started with 0% of A and linear increased to 100% of A during 20 min, and held isocratically for 35 min, returning, to the initial conditions in 5 min. The flow rate through the column was 16 μl/ min obtained using a pre-column split (Acurate, LC Packings, USA) (101).

8.1 Electrospray Mass Spectrometry Conditions

The phospholipid analysis was carried out in positive and negative modes on electrospray (ESI) linear ion trap mass spectrometer (ThermoFinnigan, San Jose, CA, USA). ESI conditions on linear ion trap mass spectrometer were as follows: electrospray voltage was 4.7 kV in negative mode and 5 kV in positive mode; capillary temperature was 275ºC and the sheath gas flow was 25 units. An isolation width of 0.5 Da was used with a 30 ms activation time for MS/MS experiments. Full scan mass spectrum and MS/MS spectrum were acquired with a 50 ms and 200 ms maximum ionization time, respectively. Normalized collision energyTM (CE) was varied between 17 and 20 (arbitrary units) for MS/MS. Data acquisition and treatment of results was carried out with an Xcalibur data System (V2.0).

9. Cell Lysate Preparation and Western Blot Analysis

To obtain the lysates for Western blot analysis, Raw cells were plated at $2x10^6$ cells/well in 6-well microplates in a final volume of 3 ml and infected with *L. infantum* promastigotes at infection ratio of 10:1 (parasite/cell) for 4 or 24 h. Cells were then washed in ice-cold PBS and harvested in RIPA lysis buffer (50 mM Tris–HCl (pH 8.0), 1% Nonidet P-40, 150 mM NaCl, 0.5% sodium deoxycholate, 0.1% SDS, 2 mM EDTA and 1 mM DTT) freshly supplemented with protease and phosphatase inhibitor cocktails (Roche, Mannheim, Germany). The nuclei and the insoluble cell debris were removed by centrifugation at 4ºC, at 12,000 *g* for 10 min. The post-nuclear extracts were collected and used as total cell lysates. Protein concentration was determined using the bicinchoninic acid method and the cell lysates were denatured at 95ºC, for 5 min, in sample buffer (0.125 mM Tris pH 6.8; 2%, w/v SDS; 100 mM DTT; 10% glycerol and bromophenol blue) for posterior use. Western blot analysis was performed to evaluate the effect of infection on

the levels of COX-1 and COX-2 in macrophages. Briefly, 30 µg of protein were separated by electrophoresis on a 12% (v/v) SDS-polyacrylamide gel, transferred to polyvinylidene fluoride (PVDF) membranes and blocked with 5% (w/v) fat-free dry milk in Tris-buffered saline, containing 0.1% (v/v) Tween-20 (TBS-T), for 1 h at room temperature. Blots were then incubated overnight at 4ºC with the primary antibodies against the COX-1(1:5000) and COX-2 (1:5000). The membranes were then washed with TBS-T and incubated, for 1 h at room temperature, with an alkaline phosphatase-conjugated anti-rabbit antibody (1:20,000). The immune complexes were detected using the Enhanced Chemifluorescence reagent and the membranes were scanned for blue excited fluorescence on the Thyphon (GE Healthcare) and analyzed using the software ImageQuant TL®. To demonstrate equivalent protein loading, membranes were stripped and reprobed with antibodies against tubulin. All the antibodies were prepared in 1% (w/v) fat-free dry milk in TBS-T.

10. RNA extraction

Cells were plated at 2 x 10^6 cells/well in 6-well microplates in a final volume of 3 ml and infected with *L. infantum* promastigotes at infection ratio of 10:1 (parasite/cell) for 4 or 24 h. Total RNA was isolated from cells with the TRIzol® reagent according to the manufacturer's instructions. Briefly, cells were washed with ice-cold PBS harvested and homogenized in 1 ml of Trizol by pipetting vigorously. After addition of 200 µl of chloroform the samples were vortexed, incubated for 2 min at room temperature and centrifuged at 12,000 g, for 15 min, at 4ºC. The aqueous phase containing RNA was transferred to a new tube and RNA precipitated with 500 µl of isopropanol for at least 10 min at room temperature. Following a 10 min centrifugation at 12,000 g, the pellet was washed with 1 ml 75% ethanol and resuspended in 100 µl 60ºC heated RNase free water. The RNA concentration was determined by OD260 measurement using a Nanodrop spectrophotometer (Wilmington, DE, USA) and quality was inspected for absence of degradation or genomic DNA contamination, using the Experion RNA StdSens Chips in the Experion™ automated microfluidic electrophoresis system (BioRad Hercules, CA, USA). RNA was stored in RNA Storage Solution (Ambion, Foster City, CA, USA) at -80ºC.

11. Real-time RT-PCR

One microgram of total RNA was reverse transcribed using the iScript Select cDNA Synthesis Kit. Briefly, 2 µl of random primers and the necessary volume of RNase-free water to complete 15 µl, were added to each RNA sample. The samples were heated at 65ºC, for 5 min, and snap-chilled on ice for 1 min. After this, 5 µl of a Master Mix containing 1 µl of iScript reverse transcriptase and 4 µl of 5x Reaction Buffer were added to each sample. A protocol for cDNA synthesis was run on all samples (5 min at 25ºC, 30 min at 42ºC, 5 min at 85ºC and then put on hold at 4ºC). After the cDNA synthesis, the samples were diluted with RNase-free water up to a volume of 100 µl. Real-time PCR was performed in a 20 µl volume containing 5 µl cDNA (50 ng), 10 µl 2x Syber Green Supermix, 2 µl of each primer (250 nM) and 1 µl H_2O PCR grade. Samples were denatured at 95ºC during 3 min. Subsequently, 40 cycles were run for 10 sec at 95ºC for denaturation, 30 sec at the appropriate annealing temperature and 30 sec at 72ºC for elongation. Real-time RT-PCR reactions were run in duplicate for each sample on a Bio-Rad My Cycler iQ5. Primers were designed using Beacon Designer® Software v7.2, from Primier Biosoft International and thoroughly tested. Primer sequences and amplification efficiencies are given in Table 1.

On each real-time PCR plate there was a non-template control present for each pair of primers analyzed. For determination of primer-pair specific efficiencies, a 4 points dilution series of control sample for each pair of primers was run on each experiment (Rasmussen, 2001). Amplification reactions were monitored using a SYBR-Green assay. After amplification, a threshold was set for each gene and Ct-values were calculated for all samples. Gene expression changes were analyzed using the built-in iQ5 Optical system software v2. The software enables analyzing the results with the Pfaffl method (Pfaffl, 2001), a variation of ΔΔCT method corrected for gene-specific efficiencies, and to report gene expression changes as relative fold changes compared to control samples. The results were normalized using a reference gene, HPRT-1, determined with Genex® software (MultiD Analyses AB) as the most stable for the treatment conditions used.

Table 1: Primer sequences for amplification using cDNA as template. The table shows the sequences of the primers used in the RT-PCR expression studies.

Gene	Primer
Mouse SCD1 FOR	5'-GTTCACTTGTAGAATCAGAG-3'
Mouse SCD1 RE	5'-CATTTCCAGAGGGCTATA-3'
Mouse SCD2 FOR	5'-TTTGACATTTAGTCTTGGT-3'
Mouse SDC2 RE	5'-TATCTCTGAGTGAGGAAG-3'
Mouse ELOVL1 FOR	5'-TTAAACTTGGGAGAGGAA-3'
Mouse ELOVL1 RE	5'-ACAGTGACAGATTATTGC-3'
Mouse ELOVL5 FOR	5'-ACCTTCTTCATCAGTTCAA-3'
Mouse ELOVL5 RE	5'-TTCCCTTTCCACAGTCTA-3'
Mouse ELOVL2 FOR	5'-TTAGCAAGACAGAATCCA-3'
Mouse ELOVL2 RE	5'-TTCATTACCACATCACTAAG-3'
Mouse ELOVL6 FOR	5'-CTCTGTTATCCTAGTTAGTCA-3'
Mouse ELOVL6 RE	5'-TTATGGCTCACGAATGTT-3'
Mouse ELOVL3 FOR	5'-ACACAACAACGGAACACT-3'
Mouse ELOVL3 RE	5'-GTGGAAGAAGTGAGCGAATA-3'
Mouse SREBF1 FOR	5'-TGTAAGGTGTATTTGCTG-3'
Mouse SREBF1 RE	5'-CAAAGGAACAACTGAGAC-3'
Mouse FASN FOR	5'-AATAGCATCATCCTCTACTTG-3'
Mouse FASN RE	5'-CTCACAGTGGTCACATAC-3'
Mouse PLA2G4A FOR	5'-GAGTTCAGAAGACATTAGAG-3'
Mouse PLA2G4A RE	5'-AAGTATTACATAATCAACATCATT-3'
Mouse PLA2G4B FOR	5'-AGAATCTGTACTGTGTAG-3'
Mouse PLA2G4B RE	5'-TGTGTAGAGATTGTAAGG-3'
Mouse PLA2G4D FOR	5'-ATTGAATACCTCCTGTGA-3'
Mouse PLA2G4D RE	5'-CTGGTGAACTGAAGATTG-3'
Mouse PLA2G4E FOR	5'-ATCTCTTGACAGTCCTCTATG-3'
Mouse PLA2G4E RE	5'-CACCTCCAGTTCTTCCAT-3'
Mouse PLA2G4F FOR	5'-CCGTGAATGCTATCTGTT-3'
Mouse PLA2G4F RE	5'-CTGTTGACAAGAGGGAAA-3'
Mouse CXCL16 FOR	5'-AAGTGAAAGCATCTTGGA-3'
Mouse CXCL16 RE	5'-GAAGTCATCTGTCTGTCT-3'
Mouse OLR1 FOR	5'-CCTTAATGTGAATGGAATAGCA-3'
Mouse OLR1 RE	5'-ACTGTGGTGGAGATGTATG-3'
Mouse MSR1 FOR	5'-TCGTCAGTCCAGGAACAT-3'
Mouse MSR1 RE	5'-ATCAAGCAGTGTCATATTCAGA-3'
Mouse COX2 FOR	5'-ATCAGACCTTCCTTGTAT-3'
Mouse COX2 RE	5'-CACACTCATAGTTAAGACA-3'
Mouse LPCAT1 FOR	5'-GAAGTTCCTGTCTCAGAT-3'
Mouse LPCAT1 RE	5'-CATATTCACGAAGGTCAAT-3'
Mouse LPCAT2 FOR	5'-TTAACCTGCCTGTATCAA-3'
Mouse LPCAT2 RE	5'-TACTTAGCCTCAGTCAAC-3'
Mouse LPCAT3 FOR	5'-ATGGGTTACTCTATGACT-3'
Mouse LPCAT3 RE	5'-TGGATATAAGGCAATATGAA-3'
Mouse LPCAT4 FOR	5'-TTTATTGTCCTCTTTCTCC-3'
Mouse LPCAT4 RE	5'-ATACAGTCTTCCTCCATC-3'

12. Determination of cytosolic PLA2 activity

The activity of calcium-dependent cytosolic phospholipase A_2 ($cPLA_2$) of RAW cells, parasites and cells infected with parasites was determines using the Cytosolic Phospholipase A_2 assay Kit (Abcam, Cambridge, UK) according to manufacturer instructions. Briefly, 5 x 10^6 macrophages, 5 x 10^8 promastigotes or 5 x 10^6 24 hours-infected cells (infection ration of 10:1 parasite/cell) where washed in PBS and resuspended in 200 µl ice cold Hepes buffer (50 mM Hepes, pH 7.4, 1mM EDTA). The cells were then sonicated five times, for 5 s at 50 µm in a Vibra Cell sonicator (Sonics & Material INC). Protein concentration was determined using the bicinchoninic acid method and 80 µg of total protein was used for each condition in the assay. 200 µl of the synthetic PLA_2 substrate arachidonoyl thio-PC were added and the plate incubated for 60 minutes at room temperature. Finally, enzyme catalysis was stopped and the reaction developed by adding 10 µl of DTNB/EGTA to each well. After 5 min incubation, the absorbance at 405 nm was read in a Multiskan 90, plate reader (Thermoscientific). PLA_2 activity for each sample was calculated according the following formula:

$$cPLA_2 \text{ Activity} = \frac{\Delta A414/min}{10.66\ mM^{-1}} \times \frac{0.225\ ml \times \text{Sample dilution}}{0.01\ ml} = \mu mol/min/ml$$

13. Immunocytochemistry

RAW cells ($4x10^4$) were plated in 12 wells µ-Chamber slides (IBIDI GmbH, Germany) and after an overnight stabilizing period were exposed for 4 hours to *L.infantum* promastigotes at a 10:1 (parasite/cell) ratio. In some experiments the phospholipase A_2 inhibitor OBAA or exogenous PLA_2 where added to cells 1h before infection. Afterwards, cells were washed three times with PBS, fixed with 4% paraformaldheyde for 15 min and washed again with PBS. The cells were then permeabilized with 0.1% (v/v) Triton-X-100, 200 mM Glycine in PBS for 10 min at room temperature. Alexa Flúor 555 Phalloidin (Molecular Probes) 1:100 in PBS was added to slides during 30 min for actin staining. After three washing steps cells were finally exposed to nuclear label DAPI (100nM) for 2 min and the slides analyzed with a fluorescent microscope (Nikon Corporation, Japan) at

630X magnification. Images were captured with a DS-Fi2 High-definition digital camera and analyzed in NIS-Elements Imaging Software (Nikon Corporation, Japan)

14. Statistical Analysis

The experiments were done independently for all conditions and the results were expressed as the means ± SD. Two way analysis of variance (ANOVA) with the Bonferroni post-hoc (for quantification of PLs and FA) was used to determine significant differences among samples. A value of $p < 0.05$ was considered significant. Statistics was done using PRISM® GraphPad Software.

III. Results

III. Results

Using a lipidomic approach, we analyzed macrophages (RAW 264.7) under 3 different conditions: macrophages without exposure to *Leishmania infantum* promastigotes (Control); macrophages exposed to formaldeide-fixed *Leishmania* promastigotes (FL) and macrophages exposed to viable *Leishmania* promastigotes (VL).

1. Macrophages phospholipid classes separation and quantification

The separation of the different phospholipid (PL) classes was accomplished by thin layer chromatography (TLC). The spots of each class were visualized after spraying with primuline, and each PL class was identified by comparison with pure standards applied in the same TLC plate. This procedure allows de fractioning and identification of lysophosphatidylcholine (LPC), sphingomyelin (SM), phosphatidylcholine (PC), phosphatidylinositol (PI), phosphatidylserine (PS), phosphatidylethanolamine (PE), cardiolipin(CL) and ceramide (CER) classes in distinct spots (Figure 7).

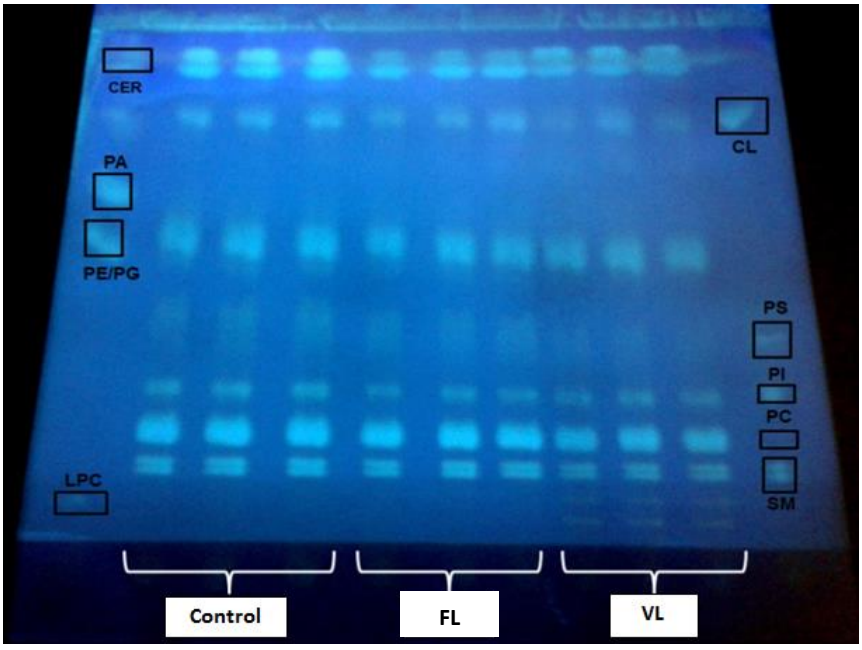

Figure 7: Thin-layer chromatography of total lipid extract from macrophages infected with viable *Leishmania* parasites (VL), macrophages exposed to fixed parasites (FL) and uninfected cells (control). Phospholipid standards were also applied: LPC, SM, PC, PI, PS, PE, PG, PA, CL and CER.

After the separation of PL classes, the phospholipid content of each TLC spot was quantified by the phosphorous assay, thereby obtaining a relative amount of each PL class in the total lipid extract (Figure 8). This analysis was carried out in duplicate for each sample in different days and for three independent biological samples (n=3).

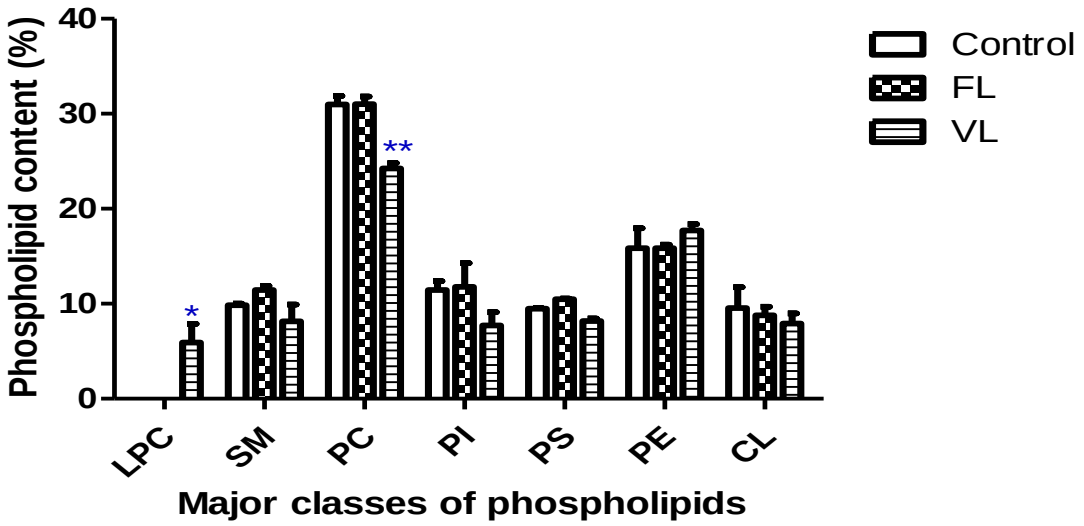

Figure 8: Major classes of phospholipids identified by TLC. In the graph is showed the relative phospholipid (PL) content (%) of PL classes in macrophages infected with viable *Leishmania* parasites (VL), macrophages exposed to fixed parasites (FL) and uninfected cell (control). Phosphate content in each spot was related to total phosphate content in the sample. In this case we were able to separate 7 different classes and quantified them: (LPC) -Lysophosphatidylcholine; (SM) - Sphingomyelin; (PC) - Phosphatidylcholine; (PI) - Phosphatidylinositol; (PS)- phosphatidylserine; (PE) - Phosphatidylethanolamine; (CL) - Cardiolipin. *p< 0.05; **p< 0.01 comparing FL and VL versus control. The graph is representative of three independent biological experiments, each one performed in duplicate (n=3).

The most abundant PL class in all conditions was PC, followed by PE. The most robust alteration between the tree conditions was found for the PC class, which was significantly decreased in cells infected with viable parasites. This decrease in PC levels was concomitantly followed by an increase in LPC class, which was only detected in macrophages exposed to viable parasites. In addition, it was possible to observe a decrease tendency in SM, PI, PS and CL phospholipid classes in the macrophages exposed to viable *Leishmania* parasites. Since the majority of the PL classes did not change significantly, this

indicates that most probably the variation of PC and LPC may be due to the action of PLA_2 (Figure 9), which converts PC in LPC.

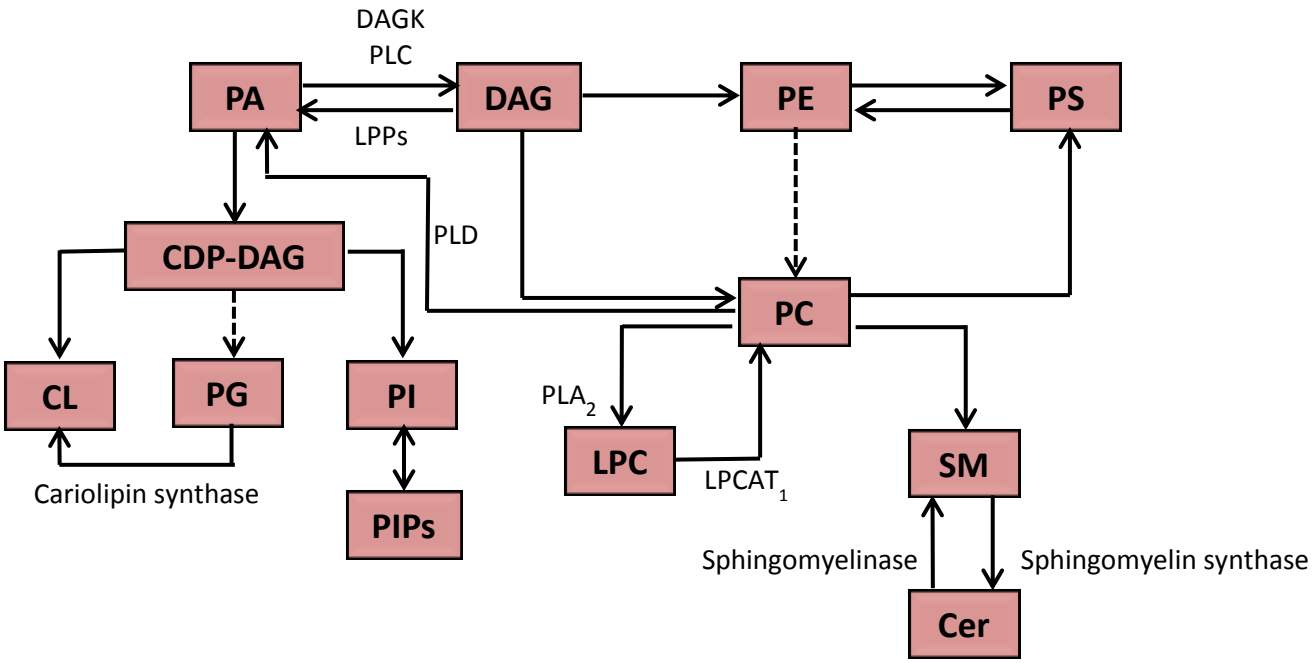

Figure 9: Schematic representation of the principal PL synthesis pathways. PLs are synthetized from PA and diacylglycerol (DAG) through different pathways and are related among them. Only the most important enzymes are displayed such as: SM synthase, Phospholipase D (PLD), Lysophosphatidylcholine acyltransferase 1 and Phospholipase A_2 (PLA_2).

2. Fatty acids analysis of macrophages

In order to evaluate a possible variation in fatty acid profile in total lipid extract of macrophages and macrophages exposed to promastigotes, the profile of fatty acids was determined by GC-FID. This procedure allowed the analysis of the fatty acids relative content in each condition under study: control, FL and VL (Figure 10). Analyses were also performed at least three times.

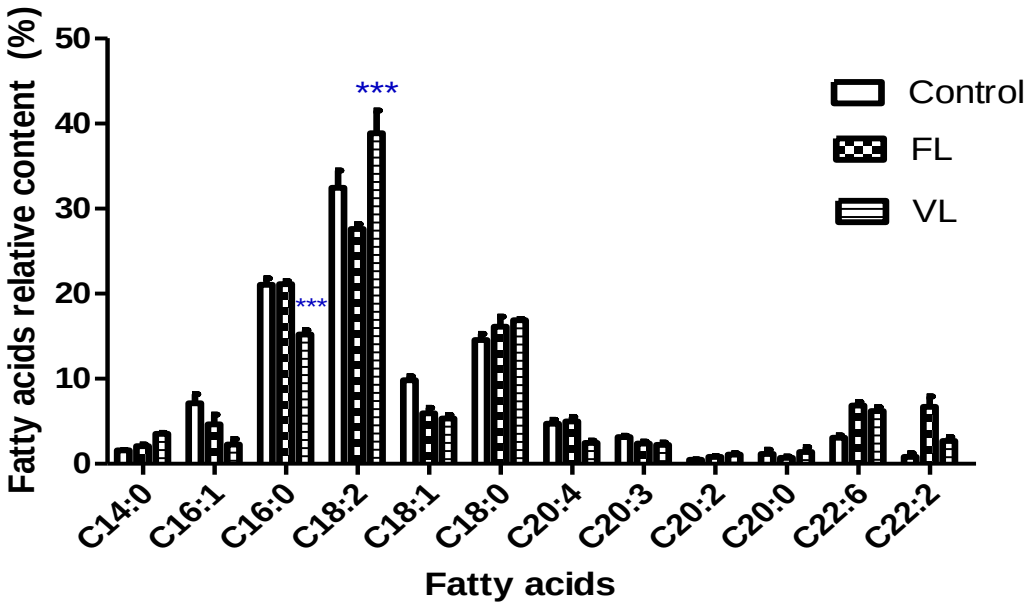

Figure 10: Relative FA content (%) in macrophages infected with viable *Leishmania* parasites (VL), macrophages infected with fixed parasites (FL) and control. We were able to identify 12 classes of FA: C14:0 (myristic acid) C16:1 (palmitoleic acid); C16:0 (palmitic acid); C18:2 (linoleic acid); C18:1 (oleic acid); C18:0 (stearic acid); C20:4 (arachidonic acid); C20:3 (eicosatrienoic acid); C20:2 (eicosadienoic acid); C20:0 (arachidic acid); C22:6 (docosahexaenoic acid); C22:2 (docosadienoic acid), *** $p < 0.01$ comparing VL versus control and FL.

Results obtained with GIC-FID allowed the identification of 12 types of distinct FA. Those with 16 and 18 carbons were predominant. Palmitic acid (C16:0) revealed to be significantly decreased only in cells infected with viable parasites while linoleic acid ($C18:2^{\Delta 9,12}$) was strongly increased in macrophages exposed to viable or fixed *Leishmania* promastigotes.

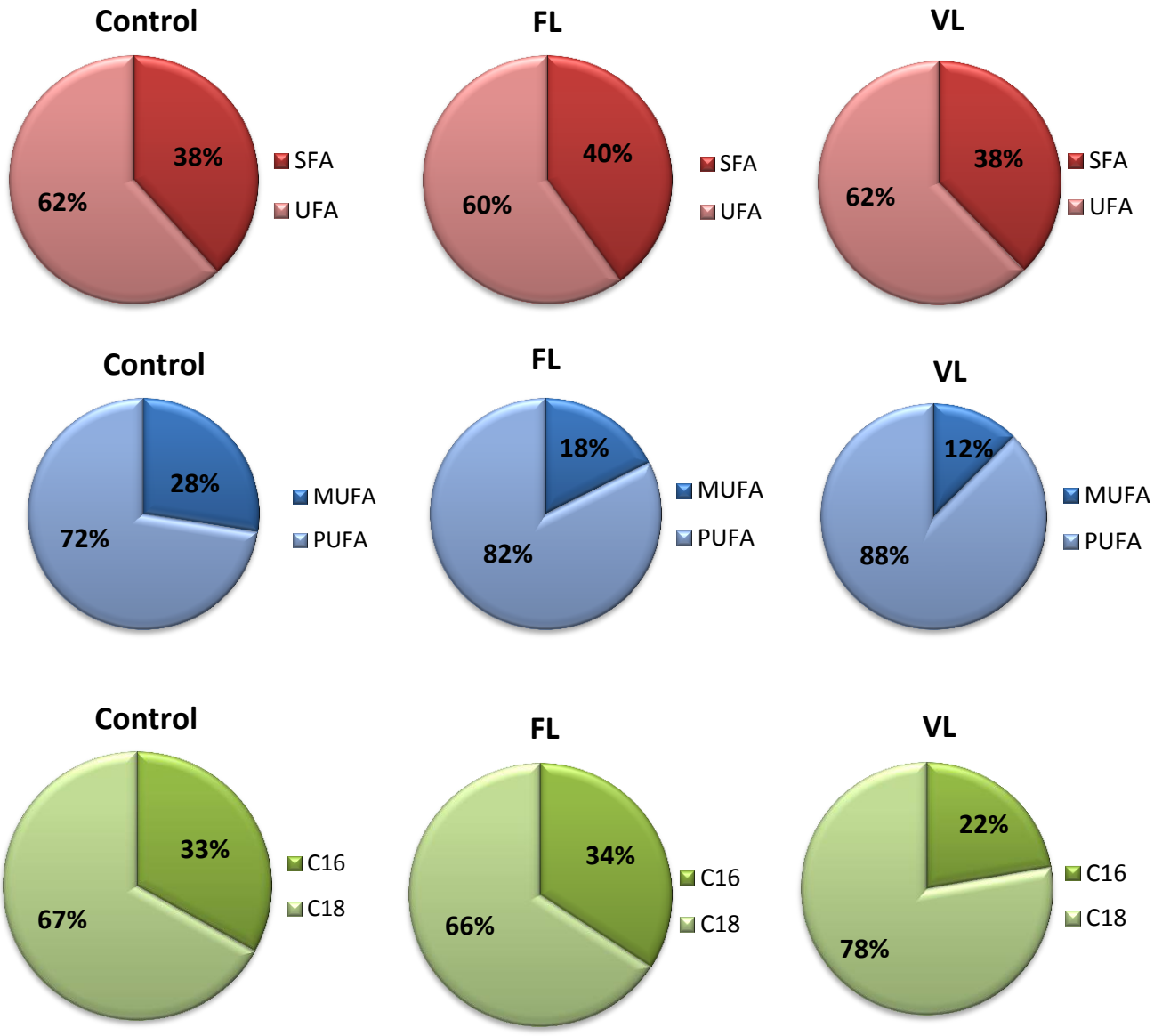

Figure 11: Analysis of fatty acid content. (A) Relationship between saturated (SFA) and unsaturated (UFA) FA; (B) between mono (MUFA) and polyunsaturated (PUFA) FA and (C) between FA with 16 and 18 carbons for the different conditions Control, FL and VL.

We proceeded to an analysis of the relationship between saturated and unsaturated FA and to the C18/C16-carbon ratio for the 12 FA groups identified. We observed that the percentages of saturated (62%) and unsaturated FA (38%) of the control and cells exposed to parasites are similar. Regarding the nature of unsaturated fatty acids, we observed a slight increase of PUFAs in cells exposed to parasites compared to Control and FL.

The major differences between the three conditions were found on the length of the chains, the percentages of FA with 16 and 18 carbons in uninfected (control) and cells exposed to fixed promastigotes (FL) are similar, while in cells infected with viable parasite (VL) we could observe a strong increase of FA with 18 carbons and a decrease of those with 16 carbons.

3. Analysis by HPLC-MS of macrophages phospholipid classes

HPLC-MS is a technique that allows the separation of PL classes and at the same time allows the analysis by MS and MS/MS of each class. The molecular species of each class were identified in order to evaluate if the changes in relative content of PL occur at the molecular level and to evaluate which PL class of macrophages is most affected by *Leishmania* promastigotes. PC, SM and LPC classes were analyzed by HPLC-MS and MS/MS in the positive mode, on the other hand, PE, PA, PS, PI e CL were analyzed by HPLC-MS and MS/MS in the negative mode. The chromatogram showing the elution of each PL class is shown in Figure 12.

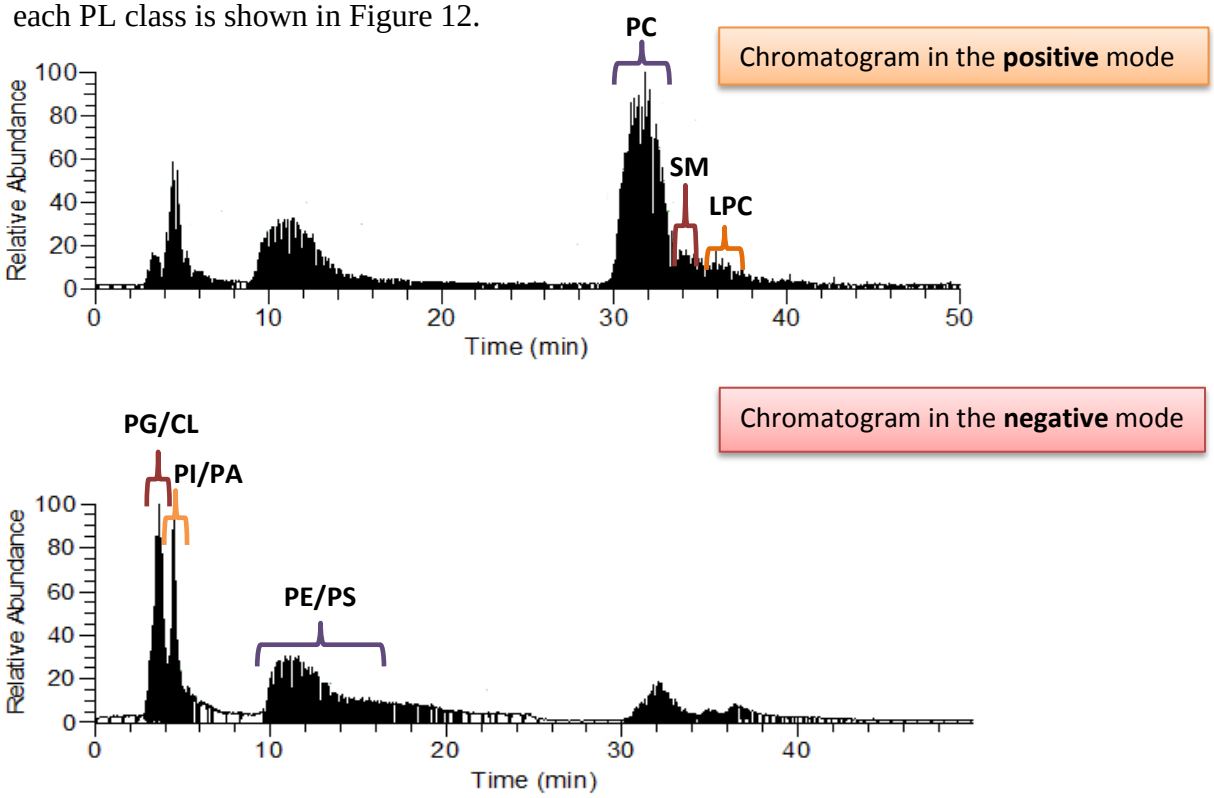

Figure 12: LC-MS Chromatograms in positive and negative modes, showing where each PL class eluted, in the mode where they were analyzed. This chromatogram was obtained from the macrophages without exposure to promastigotes (Control) and is shown as an example since all the chromatograms had a similar profile.

3.1 Analysis of PC profile

PCs ionize preferentially in the positive mode, forming $[MH]^+$ ions in the MS spectra. In Figure 13 it is shown the HPLC-MS spectra for the PC profiling obtained for the three conditions. The confirmation of the presence of PC molecular species, theirs most probable composition in fatty acyl chains and possible location in the glycerol backbone was accomplished by MS/MS. The MS/MS analysis of PCs shows a characteristic product ion at *m/z* 184, another product ion due to neutral loss of polar head (loss of 183) and ions due to loss of the fatty acyl chains as represented in Figure 14 (102). We were able to identify two groups of molecular species: diacyl-PC and alkenyl-PC (Figure 15).The most abundant PC species identified are summarized in Table 2.

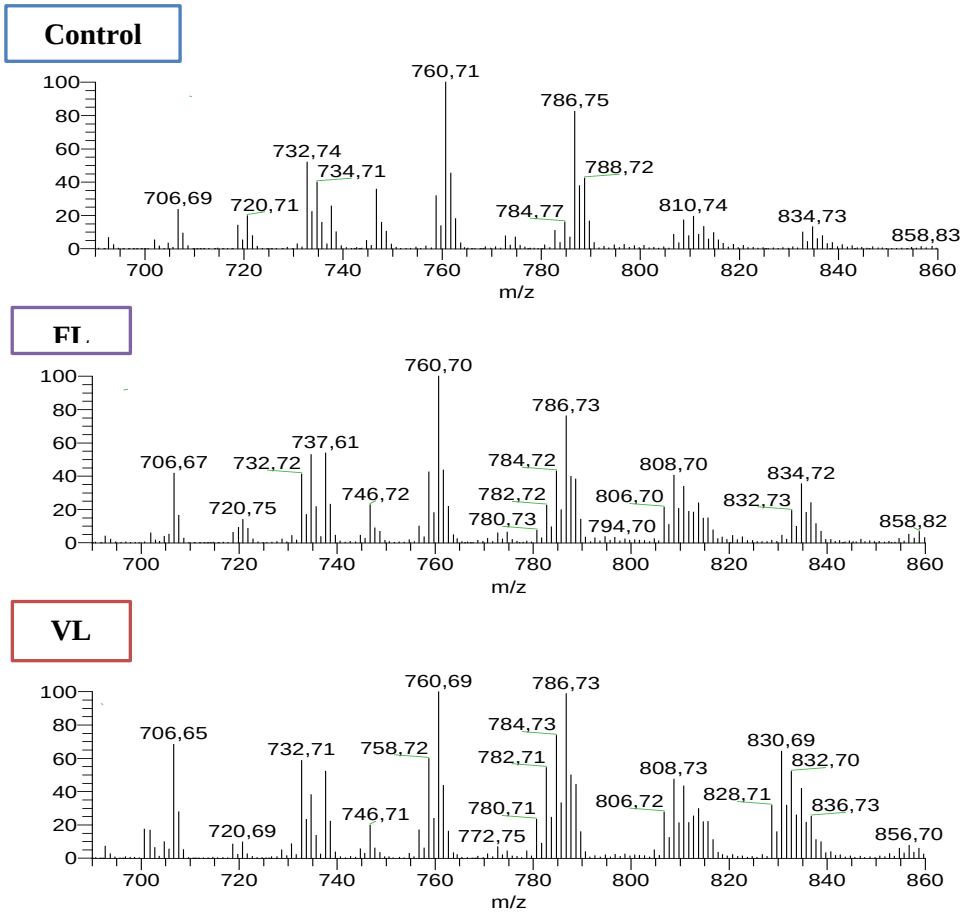

Figure 13: HPLC-MS spectra of PC class in the positive mode with formation of $[MH]^+$ ions, in control (Control), macrophages exposed to fixed promastigotes (FL) and macrophages exposed to viable promastigotes (VL). Y-axis: Relative abundance considering the highest abundant ion as 100 %; x-axis: *m/z* for each ion

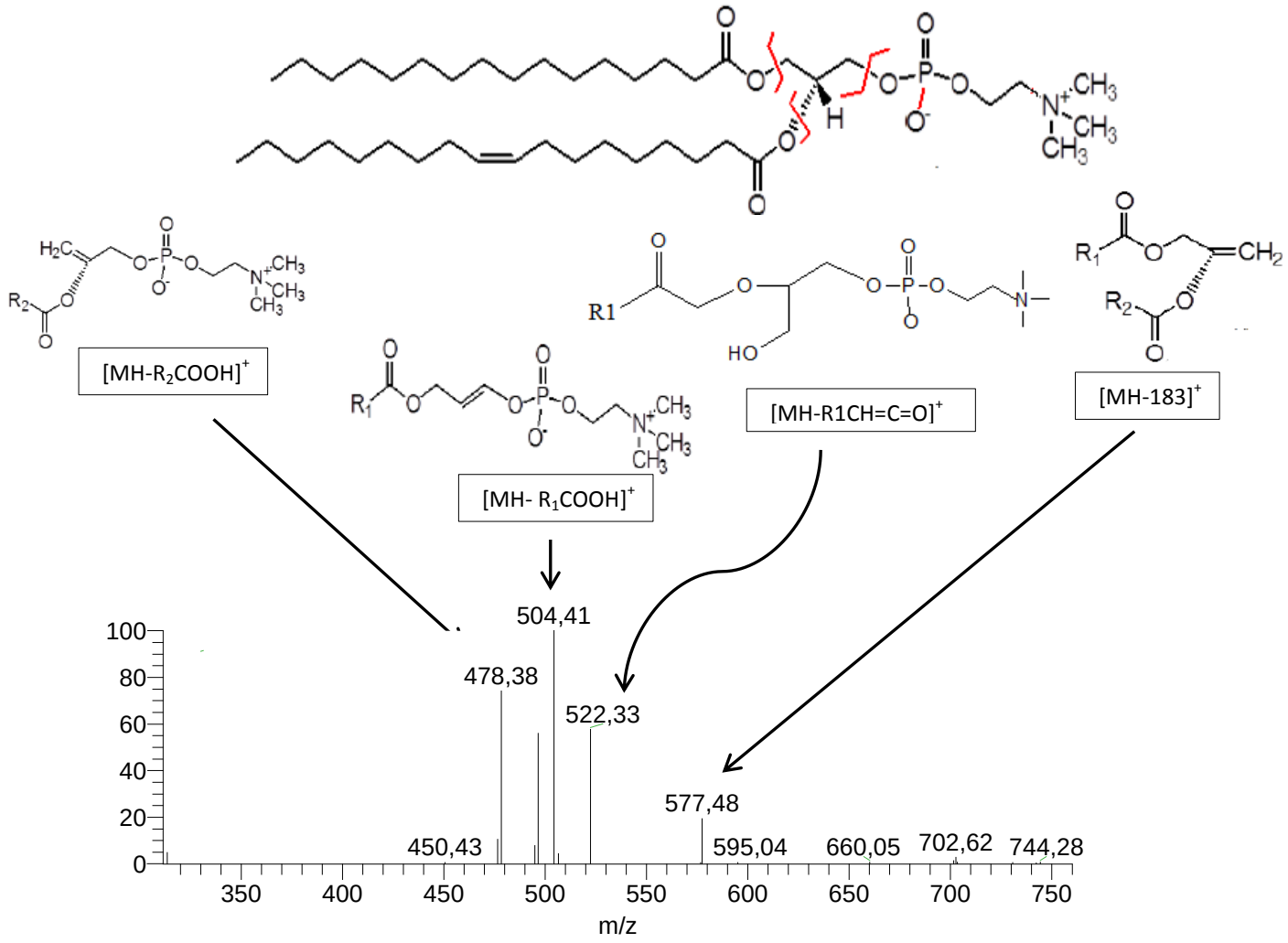

Figure 14: MS/MS spectrum of PC $[M+H]^+$ at *m/z* 760.7 (PC C16:0/18:1) with the fragmentation patterns of PCs.

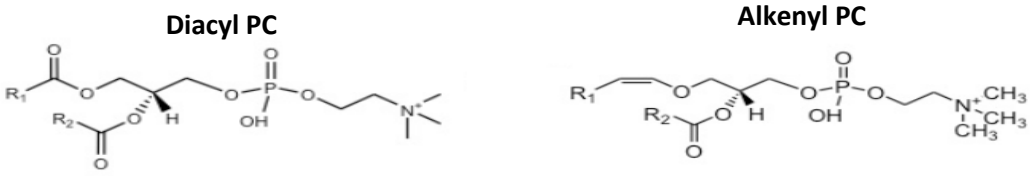

Figure 15:General structure of diacyl and plasmenyl PC class.

Table 2: Identification of $[MH]^+$ ions observed in the MS spectra in PC; p - an sn-1 vinyl ether (alkenyl- or plasmalogen) linkage.

	Dyacil Species		
Classe	***m/z* [MH]$^+$**	**C:N**	**Fatty Acyl Chains**
PC	**706.6**	**30:0**	**14:0/16:0**
	732.7	**32:1**	**14:0/18:1 16:0/16:1**
	734.7	**32:0**	**16:0/16:0 14:0/18:0**
	758.7	34:2	16:0/18:2
	760.7	**34:1**	**16:0/18:1**
	780.7	36:5	16:1/20:4
	782.7	36:4	18:2/18:2
	784.7	36:3	18:1/18:2
	786.7	**36:2**	**18:0/18:2**
	806.7	38:5	16:0/22:6
	806.7	38:6	18:2/20:4
	808.7	38:5	18:1/20:4
	810.7	**38:4**	**18:0/20:4**
	812.7	38:3	18:0/20:3
	814.7	38:2	18:1/20:1
	836.7	40:5	20:1/20:4
	830.7	40:8	18:2/22:6
	832.7	40:7	18:1/22:6
	834.7	40:6	18:0/22:6
Alkenyl Species			
	718.7	32:0p	16:0p/16:0

Attribution of the fatty acyl composition of each PC molecular species was done accordingly to the interpretation of the correspondent MS/MS spectra. C: number of carbons in the fatty acid chain and N: number of double bonds.

As it can be seen in the Figure 13, the HPLC-MS spectra are similar for the three conditions considering the ions with higher relative abundance were the ones with *m/z* values of: 706.6; 732.7: 734.7; 760.7 and 786.7 7. However, differences were observed for the PC ions at *m/z* values of: 828.7 (PC 18:3/22:6), 830.7 (PC 18:2/22:6), which presented a higher relative abundance in macrophages exposed to viable *Leishmania* parasites (VL). In fact, these data are in accordance with data of fatty acyl profile, since in at m/z 830 has a C18:2 that was increase in the profile of macrophages infected with *L. infantum*. 782.7 and 784.7, PC species with C18:2 were also increase in the infected macrophages. The spectra also demonstrated that the ion *m/z* 786.7 presented a higher relative abundance in the VL condition.

3.2. Analysis of SM profile

SM species ionize in MS in positive mode as $[MH]^+$, similar to PC. Thee MS/MS spectra showed also the typical choline phosphate product ion at *m/z* 184. They can be easily differentiated from PC, since $[MH]^+$ ions of PC appear at even *m/z* values, whereas $[MH]^+$ ions of SM exhibit odd *m/z* values due to the presence of an additional nitrogen atom in SM. The major SM molecules identified are resumed in Table 3.

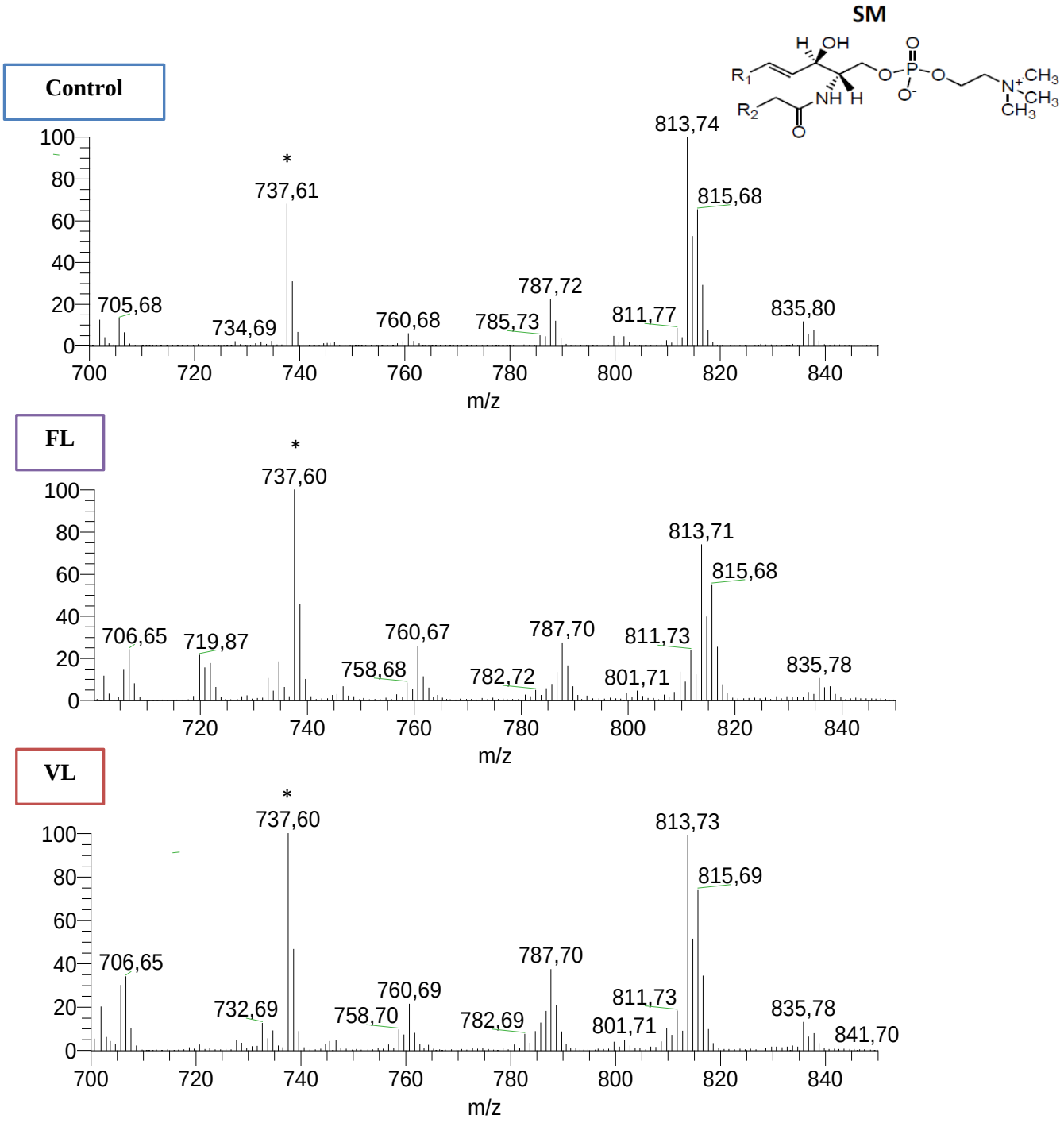

Figure 16: **General structure of SM class; HPLC-MS spectra of SM class in the positive mode with formation of $[MH]^+$ ions, in control (Control), macrophages exposed to fixed promastigotes (FL) and macrophages exposed to viable promastigotes (VL).**Y-axis: Relative abundance considering the highest abundant ion as 100 %; x-axis: *m/z* for each ion. *737.6 peak correspondent to the eluent.

Table 3: Identification of $[MH]^+$ ions observed in the MS spectra in SM.

	Dyacil Species		
Classe	***m/z* [MH]$^+$**	**C:N**	**Fatty Acyl Chains**
SM	**705.4**	**34:0**	**d18:0/16:0**
	785.7	40:2	d18:1/22:1
	787.7	**40:1**	**d18:0/22:1**
	789.7	40:0	d18:0/22:0
	811.7	42:3	d18:1/24:2
	813.7	42:2	d18:1/24:1
	815.7	42:1	d18:1/24:0
	817.7	42:0	d18:0/24:0
	835.7	44:5	d18:1/26:4

Attribution of the fatty acyl composition of each SM molecular species was done accordingly to the interpretation of the correspondent MS/MS spectra. C: number of carbons in the fatty acid chain and N: number of double bonds.

As it can be seen in the Figure 14, the HPLC-MS spectra are similar for the three conditions, except for the ion with *m/z* value of 705.4, which the relative is increased in the macrophages exposed to viable *Leishmania* parasites (VL).

3.3 Analysis of LPC profile

The LPC class was only detect in TLC in macrophages exposed to viable *Leishmania* promastigotes (VL), however we were able to identify some ions of this class in HPLC-MS in Control and FL. LPCs were analyzed in the positive ion mode, with the formation of $[MH]^+$ ions that were identified in the HPLC-MS spectra. The major LPC molecules identified are resumed in Table 4.

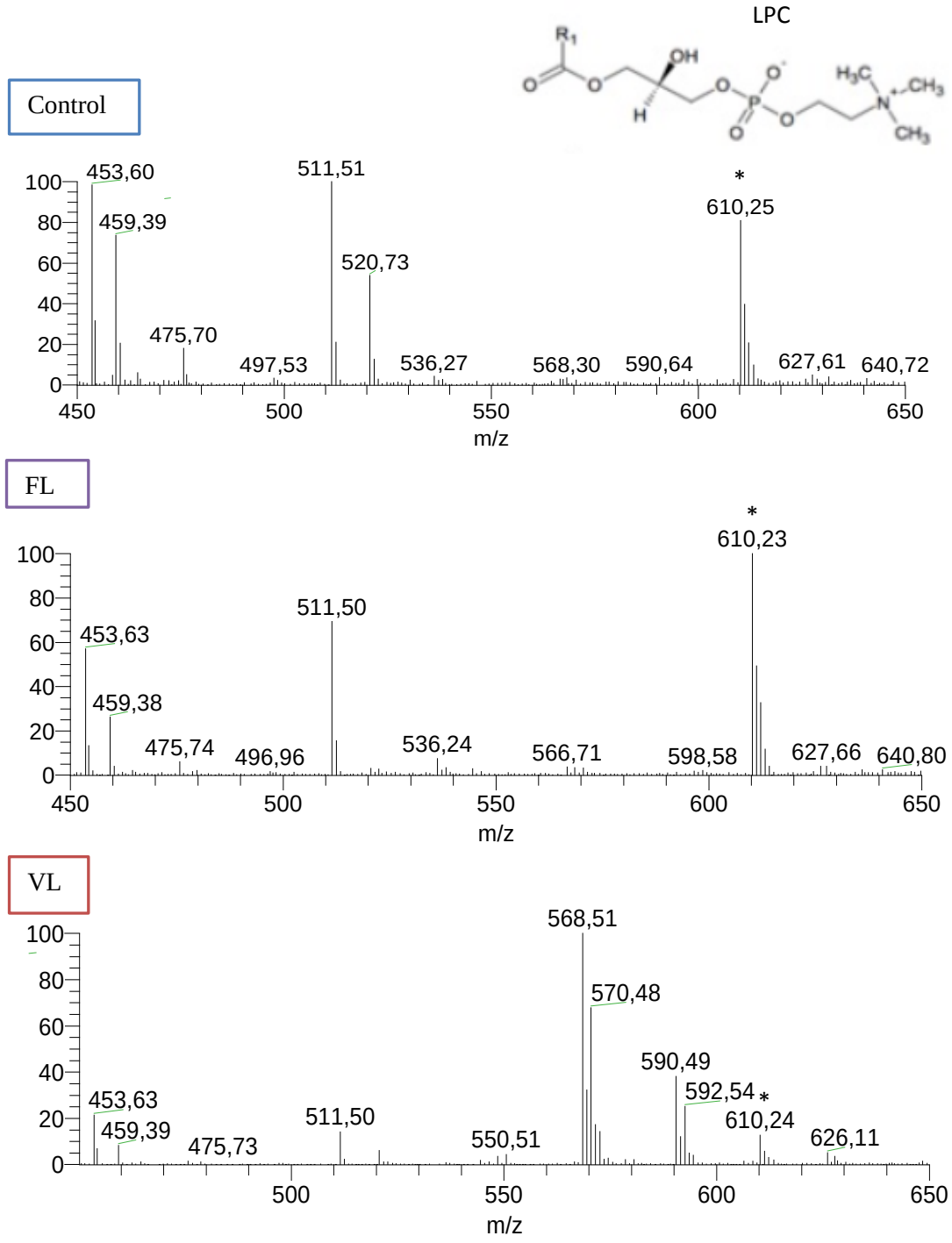

Figure 17: General structure of LPC class; HPLC-MS of LPC class in the positive mode with formation of $[MH]^+$ ions, in control (Control), macrophages exposed to fixed promastigotes (FL) and macrophages exposed to viable promastigotes (VL). Y-axis: Relative abundance considering the highest abundant ion as 100 %; x-axis: *m/z* for each ion.*610.2 correspondent to the eluent.

Table 4: Identification of $[MH]^+$ ions observed in the MS spectra in LPC.

.

	Monoacyl Species	
Classe	***m/z* [MH]$^+$**	**C:N**
LPC	520.7	18:2
	568.5	22:6
	570.4	22:5

Attribution of the fatty acyl composition of each LPC molecular species was done accordingly to the interpretation of the correspondent MS/MS spectra. C: number of carbons in the fatty acid chain and N: number of double bonds.

The analysis of the HPLC-MS spectra in the LPC region for the different conditions demonstrated that the molecular species with *m/z* values of 568.5 and 570.4 only were detected in the macrophages exposed to viable *Leishmania* promastigotes (VL).

The ions at *m/z* 590 and 592 detected in the LC-MS in the case of infected macrophages were identified as sodium adducts of each above described LPC species.

3.4 Analysis of PE profile

The molecular species of PE class were analyzed in the HPLC-MS in negative mode by the formation of $[M-H]^-$ ions (Figure 18) . The most abundant PE molecules identified are summarized in Table 5. PE species identified included two groups of molecular species: diacyl-PE and alkenyl-PE (Figure 19).

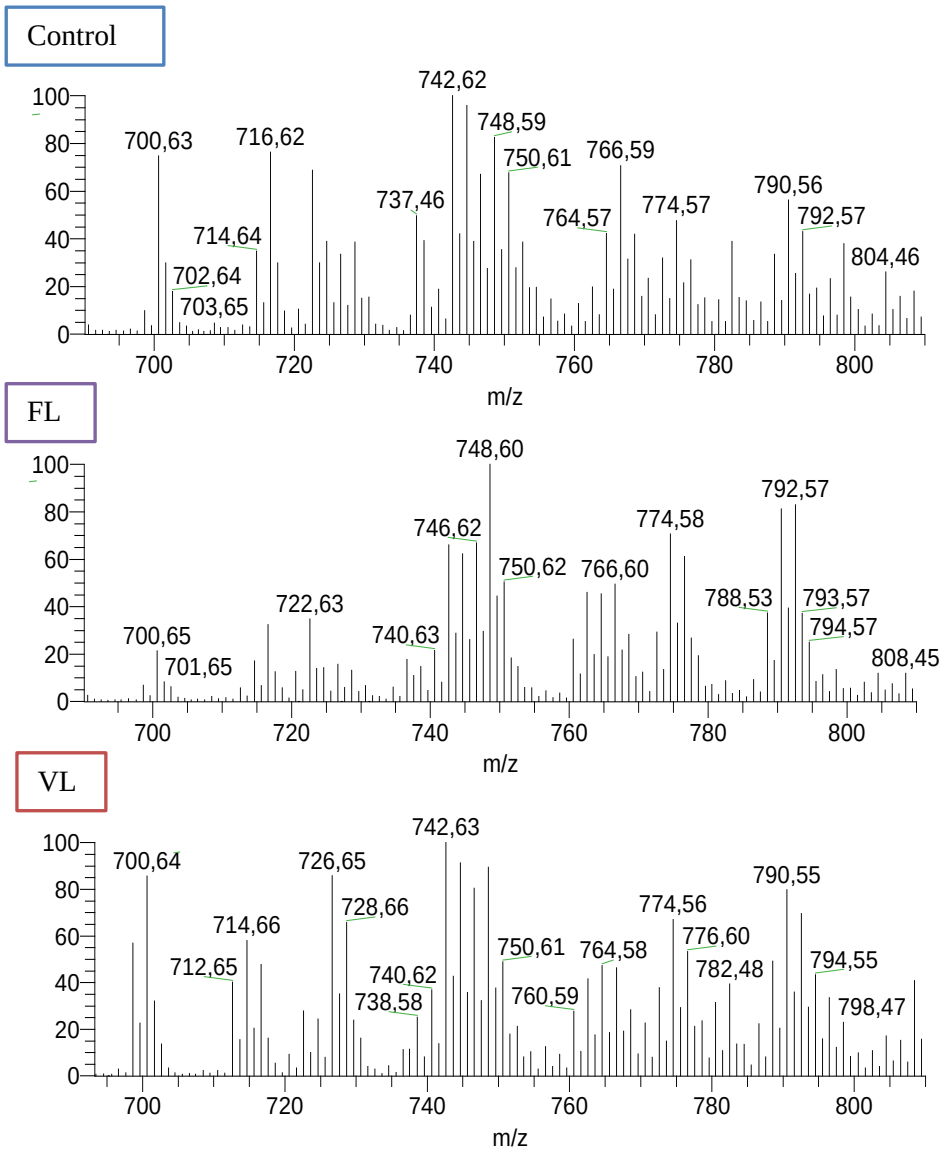

Figure 18: HPLC-MS spectra of PE class in the negative mode with formation of [M-H]$^-$ ions, in control (Control), macrophages exposed to fixed promastigotes (FL) and macrophages exposed to viable promastigotes (VL). Y-axis: Relative abundance considering the highest abundant ion as 100 %; x-axis: *m/z* for each ion.

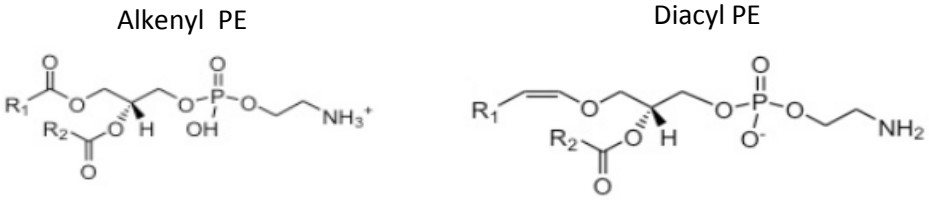

Figure 19: General structure of diacyl PE and alkenyl PE.

Table 5: Identification of [M-H]- ions observed in the MS spectra of PE; p - an sn-1 vinyl ether (alkenyl- or plasmalogen) linkage..

	Diacyl Species		
Classe	***m/z* [M-H]$^-$**	**C:N**	**Fatty acyl chains**
PE	**714.6**	**34:2**	**16:0/18:2** **16:1/18:1**
	716.6	**34:1**	**16:0/18:1** **16:1/18:0**
	740.6	36:3	18:1/18:2 18:0/18:3
	742.6	**36:2**	**18:1/18:1**
	744.5	**36:1**	**18:0/18:1**
	746.6	36:0	18:0/18:0
	762.5	38:6	16:0/22:6
	764.5	38:5	18:0/20:5 18:1/20:4
	766.6		**18:0/20:4**
	768.4	38:3	18:0/20:3 18:1/20:2
	790.5	**40:6**	**18:0/22:6**
	792.5	**40:5**	**18:1/22:4** **18:0/22:5**
	794.5	40:4	18:0/22:4 18:1/22:3
	796.4	40:3	18:0/22:3
	798.5	40:2	18:0/22:2 18:1/22:1
	Alkenyl Species		
	700.6	34:2p	16:0p/18:2 16:1p/18:1
	702.5	34:1p	16:0/18:1 16:1/18:0
	722.6	36:4p	16:0p/20:4
	724.6	36:3p	18:1p/18:2
	726.6	36:2p	18:0p/18:2
	728.6	36:1p	18:0p/18:1
	774.5	**40:6p**	**18:0p/22:6**
	776.4	40:6p	18:1p/22:5

Attribution of the fatty acyl composition of each PE molecular species was done accordingly to the interpretation of the correspondent MS/MS spectra. C: number of carbons in the fatty acid chain and N: number of double bonds.

The ions with a higher relative abundance in the Control, FL and VL were the ones at *m/z* 714.6; 716.6; 742.6; 744.5; 766.6; 790.5; 792.5 and 774.5. Comparing the HPLC-MS spectra of the three different conditions it can be seen that *Leishmania* promastigotes only caused a decrease of the relative abundance in the molecular specie at m/z value of: 766.6 and an increase of the molecular species with *m/z* values of 726.6, 728.6792.5 and 798.5.

3.5 Analysis of PS profile

PS molecular species were also analyzed by HPLC-MS in the negative mode, showing $[M-H]^-$ ions (Figure 20). In PS mass spectra we only were able to identify diacyl-species. PS species identified are presented in Table 6.

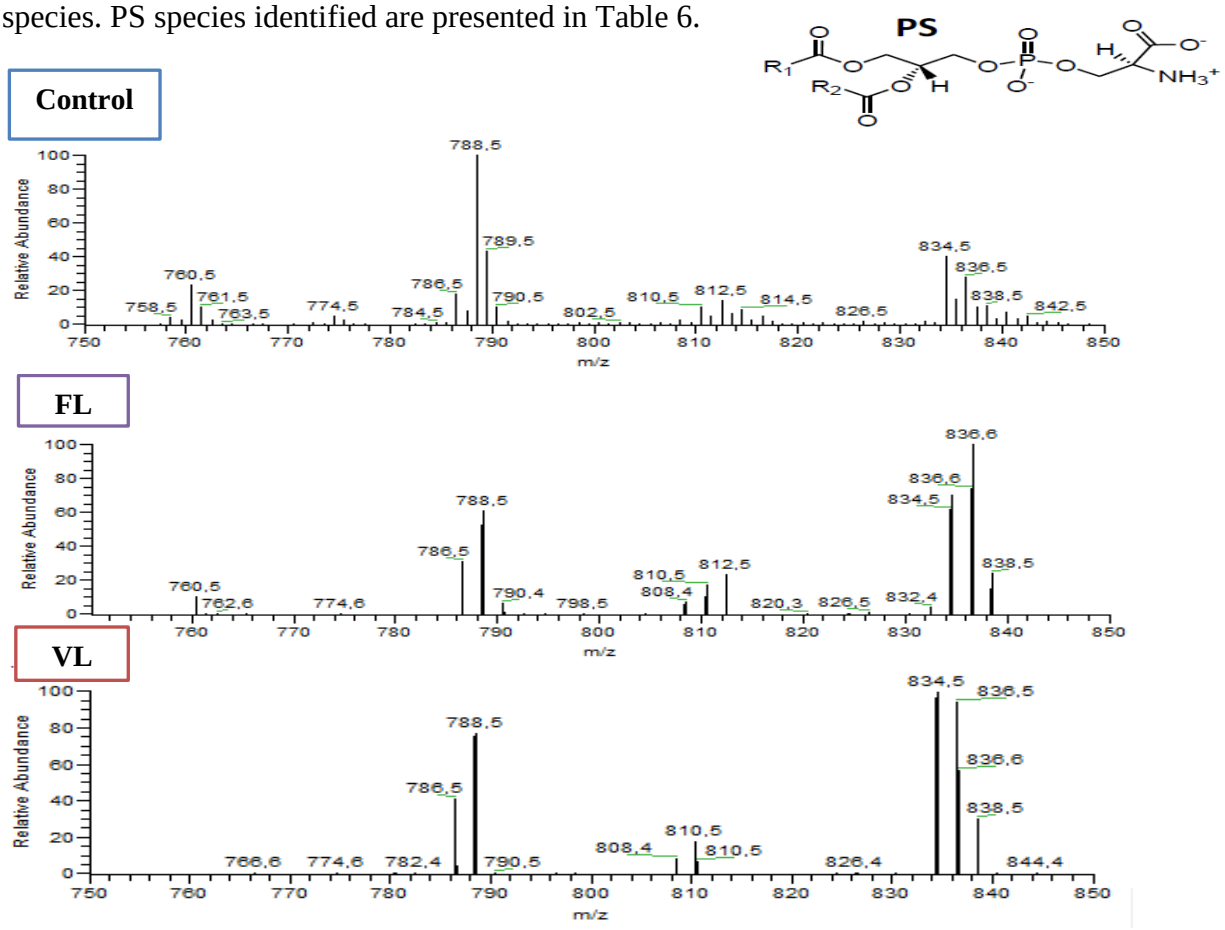

Figure 20: General structure of PS class; HPLC-MS spectra of PS class in the negative mode with formation of $[M-H]^-$ ions, in control (Control), macrophages exposed to fixed promastigotes (FL) and macrophages exposed to viable promastigotes (VL). Y-axis: Relative abundance considering the highest abundant ion as 100 %; x-axis: *m/z* for each ion.

Fragmentation observed in MS/MS spectra of the $[PS-H]^-$ ions showed a typical neutral loss of 87 Da due to loss of serine moiety, and also carboxylate ions RCOO-, that allowed the identification of the PS molecular composition. As an example we show in Figure 21 the MS/MS spectrum of the PS molecular species with $[M-H]^-$ ion at *m/z* 788.5, where we can see that *m/z* 701 the product ion $[PS-H87]^-$, which corresponds to the loss of the serine group and the carboxylate ions at *m/z* 281 and 283, which corresponds to the C18:1 and C18:0 fatty acyl chains, allowing the identification of this PS specie as PS (18:0/18:1).

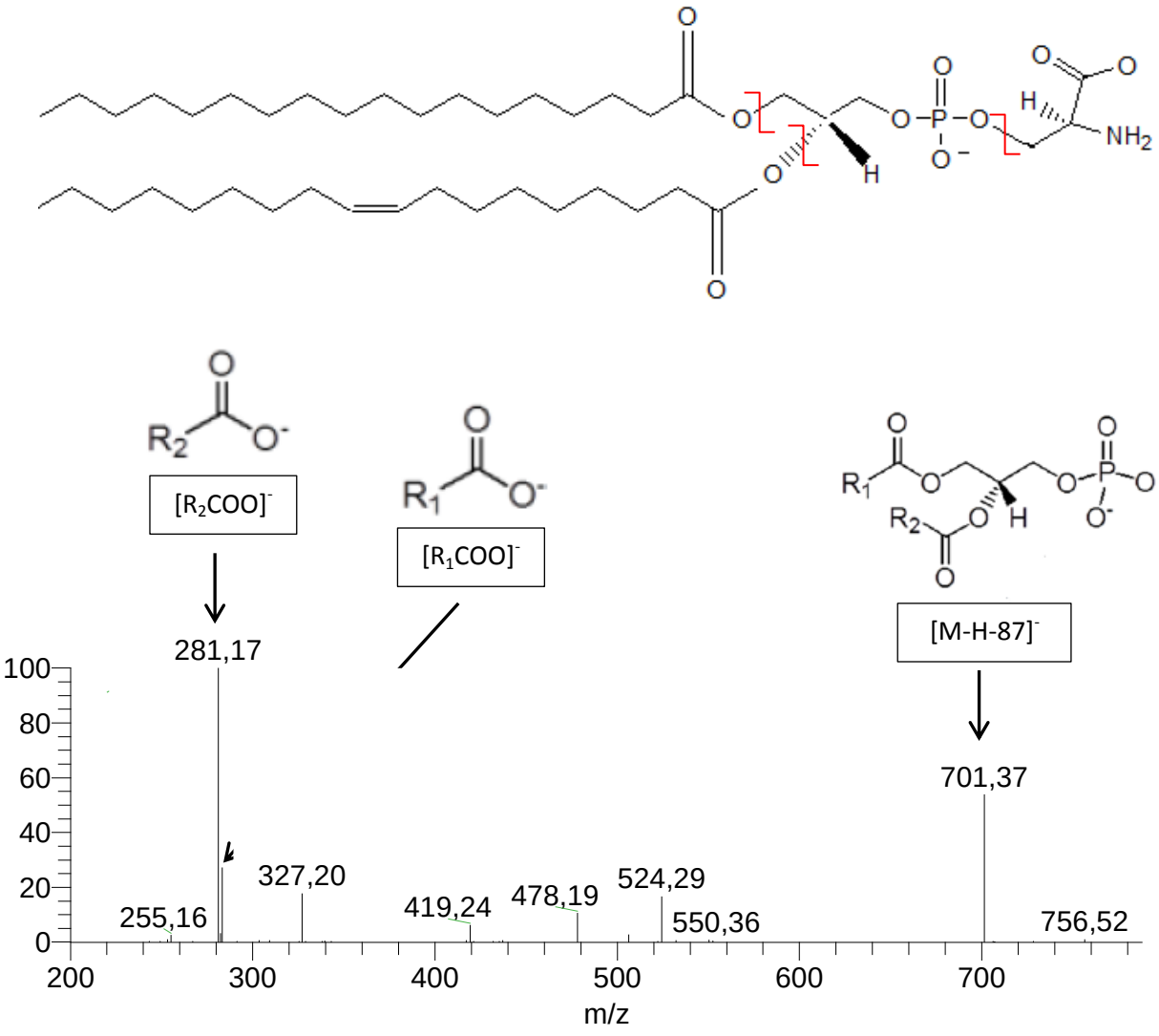

Figure 21: MS/MS spectrum of the $[M-H]^-$ at *m/z* 788.6 correspondent to the PS C18:0/18:1, with the indication of the main fragmentation patterns of PSs.

Table 6: Identification of $[M-H]^-$ ions observed in the MS spectra of PS.

Classe	*m/z* [M-H]-	C:N	Fatty acyl chains
PS	758.5	34:2	16:0/18:2
	760.5	34:1	16:0/18:1
	786.5	36:2	18:1/18:1
	788.5	36:1	18:0/18:1
	790.4	36:0	18:0/18:0
	808.5	38:5	18:1/20:4 18:2/20:3
	810.5	38:4	18:0/20:4 18:1/20:3
	812.5	38:3	18:0/20:3
	832	40:7	18:1/22:6
	834.5	40:6	18:0/22:6
	836.6	40:5	18:0/22:5
	838.5	40:4	18:0/22:4

Attribution of the fatty acyl composition of each PS molecular species was done accordingly to the interpretation of the correspondent MS/MS spectra. C: number of carbons in the fatty acid chain and N: number of double bonds.

As it can be seen in the figure 20, the molecular species with higher relative abundance in the three conditions were 786.5; 788.5; 834.5 and 836.6. The species with $[M-H]^-$ ions at *m/z* 760.5 and 812.5 were only detected in Control and FL. On the other hand, the molecular species at *m/*z values of 834.5 PS (18:0/22:6) is significantly increased in VL.

3.6 Analysis of PI profile

PIs were analyzed also in the negative mode forming $[M-H]^-$ ions in the HPLC-MS spectra. The identified PI molecules are resumed in Table 7.

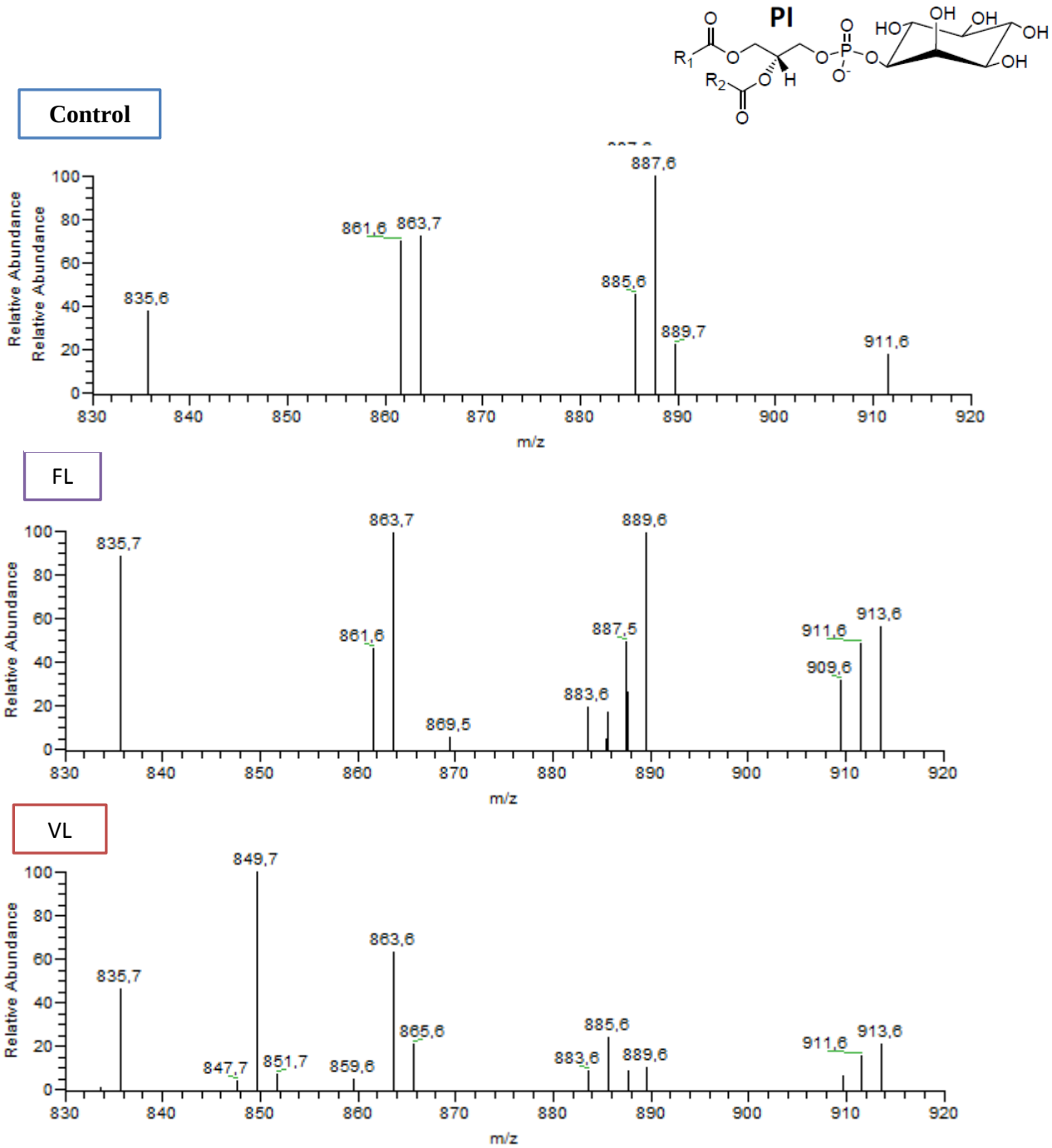

Figure 22: General structure of PI class; HPLC-MS spectra of PI class in the negative mode with formation of $[M-H]^-$ ions, in control (Control), macrophages exposed to fixed promastigotes (FL) and macrophages exposed to viable promastigotes (VL). Y-axis: Relative abundance considering the highest abundant ion as 100 %; x-axis: *m/z* for each ion.

Table 7: Identification of $[M-H]^-$ ions observed in the MS spectra of PI.

Classe	*m/z* [M-H]-	C:N	Fatty acyl chains
PI	835.6	34:1	16:0/18:1 16:1/18:0
	861.6	36:2	18:1/18:1 18:0/18:2
	863.6	36:1	18:1/18:0
	883.6	38:5	18:1/20:4 18:0/20:5
	885.5	38:4	18:0/20:4 18:1/20:3
	887.6	38:3	18:0/20:3 18:1/20:2
	889.7	38:2	18:0/20:2 18:1/20:1
	911.5	40:5	18:0/22:5 18:1/22:4

Attribution of the fatty acyl composition of each PI molecular species was done accordingly to the interpretation of the correspondent MS/MS spectra. C: number of carbons in the fatty acid chain and N: number of double bonds.

Comparing the HPLC-MS spectra of the three conditions, we can see that the molecular species with *m/z* values of 861.6 and 887.6 were not detected in VL. The molecular species with *m/z* values of 885.5 and 889.7 presented a lower relative abundance in VL.

4. Expression analysis using RT-PCR

The effects of parasites on the transcription of genes related to macrophage lipid metabolism were analyzed by quantitative RT-PCR (Table 8). In order to confirm and elucidate results obtained in TLC and GC analysis, selected genes include fatty acid desaturases and elongases and several enzymes related to PC-LPC interconversion such as phospholipase A_2 and LPCAT.

Table 8: Gene expression profile of macrophages exposed to viable *Leishmania* (VL) and fixed *Leishmania* (FL) after 4 and 24 hours of exposure.

Gene	Fold expression (4h of exposure)		Fold expression (24h of exposure)	
	VL	FL	VL	FL
ABCA1	0,915	0,595	**0,305**	0,88
ABCG1	1,035	0,5	0,72	0,72
FABP4	**3,05**	2,65	**8,71**	3,65
CD36	0,96	2,1	1,06	1,275
CXCL16	1,2	1,3	0,99	0,75
MSR1	1,1	1,1	1,97	1,29
OLR1	2,3	2,3	1,93	0,86
PLA2G4A	1,04	1,16	0,87	0,85
PLA2G4B	0,75	0,79	0,76	0,6
PLA2G4D	ND	ND	ND	ND
PLA2G4E	ND	ND	ND	ND
PLA2G4F	**3,2**	1,4	0,65	0,45
FASN	0,61	0,98	**0,31**	0,86
SREBF	0,73	1,41	1,14	0,7
SCD1	0,97	1,06	1,21	0,52
SCD2	0,85	0,59	1,13	0,7
ELOVL1	0,78	1,05	0,74	0,63
ELOVL2	**4,7**	1,47	0,86	0,22
ELOVL3	0,93	1,31	0,43	0,76
ELOVL5	1,41	1,52	0,76	0,88
LPCAT1	1,1	1,8	1	0,91
LPCAT2	1,1	1,7	1,05	0,93
LPCAT3	1,6	1,8	0,82	0,88

The values represent the fold changes relatively to uninfected cells. When the expression was not detected the designation is ND.

As shown in Table 8, several lipid metabolism-related genes were altered after macrophage exposure to viable or fixed parasites. From our results, the expression of LPCAT enzymes was not significantly modulated by exposure of cells to either viable or

fixed parasites. Regarding the analysis of genes coding cytosolic phospholipase A_2 we observed that PLA_2G4A, PLA_2G4B and PLA_2G4F were constitutively expressed, while PLA_2G4D and PLA_2G4E were barely detected in RAW cells. Among PLA_2 isoforms only PLA_2G4F revealed to be modulated by parasites: viable promastigotes caused an early increase in PLA_2G4F mRNA and by contrast fixed parasites caused a slight decrease after 24h (Table 8). PLA_2 are enzymes that specifically recognize the sn-2 acyl bond of phospholipids and catalytically hydrolyze the bond releasing arachidonic acid and lysophospholipids. Therefore, this observation could somehow partially explain our previous results where higher levels of LPC were detected in cells infected with viable promastigotes. Additionally, we found an increased level of elongase ELOVL2 mRNA exclusively in viable parasite-infected cells. Once again this could partially explain the increased fatty acid C18/C16 ratio observed in macrophages exposed to viable promastigotes. Other lipid-metabolism related genes substantiality modulated by infection are FASN and FABP4. Transcription of fatty acid synthase (FASN) is markedly decreased while fatty acid binding protein 4 is increased after 24h of exposure. FASN gene encodes a multifunctional enzyme that catalyzes the synthesis of palmitate from acetyl-CoA and malonyl-CoA. Therefore these results support our previous observation in which infected cells presented decreased levels of palmitic acid. Finally, among analyzed genes we also observed after 24h exposure to viable promastigotes a marked decrease in the mRNA levels of cholesterol efflux transporter ABCA1 suggesting a disruption in cells ability to remove cholesterol from its cytoplasm.

5. Western blot analysis of COX-1 and COX-2

Given that we found increased levels of LPC in infected-macrophages suggesting and increase activity of PLA_2 enzymes we hypothesize that a possible concomitant increase in arachidonic acid could cause changes in cyclooxygenase protein expression. Therefore, we analyzed by Western blot the expression of COX-1 and COX-2 proteins in cells exposed to viable or fixed parasites. As a positive control for COX-2 induction we treated macrophages with *E. coli* O157 lipopolysaccharide (LPS).

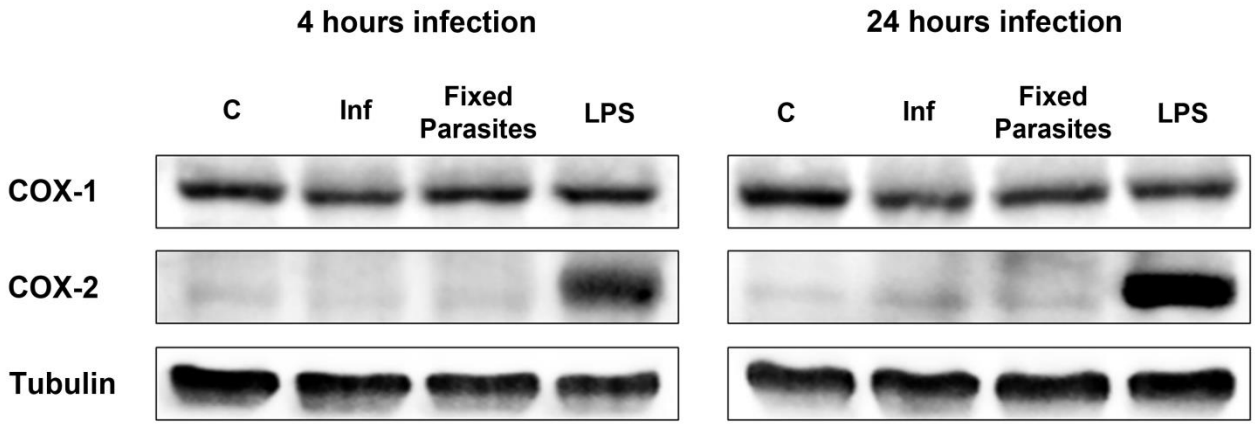

Figure 23: Effect of infection on the macrophages expression of COX-1 and COX-2. RAW cells ($3x10^6$ per well of a 6 well plate) were exposed to viable (Inf) or fixed *L. infantum* promastigotes in a cell/parasite ratio of 1:10. Cell lysates were prepared after 4 or 24 hours of infection. As a positive control, macrophages were stimulated with 1 µg/ml of LPS during the indicated periods. 30 µg of protein were loaded on a 12% SDS-polyacrylamide gel and expression of COX-1 and COX-2 examined by Western blot using specific antibodies. The optical densities of the bands were obtained by scanning the membranes in a fluorescence scanner, and then analysed with the ImageQuant TL Software. The results are representative of three independent experiments. Equal protein loading between samples was controlled by stripping and reprobing membranes with β-Tubulin antibody.

As it can be seen in Figure 23, exposure of macrophages to either viable or fixed parasites does not induce noticeable changes in COX-1 and COX-2 expression. In contrast, and as expected, we observed a marked increase in COX-2 protein levels in cells treated with LPS.

6. PLA_2 activity assay

We previously showed in this work that cells infected with viable promastigotes present increased levels of lisophosphatidilcholine, and that this observation could be partially explained by an increased expression of PLA_2G4F. However it is also plausible that infection causes an increase in the macrophage PLA_2 family activity or that parasites possess intrinsic PLA_2-like activity. To address this question we analyzed the total and

cytosolic PLA_2 activity of macrophages, *L.infantum* promastigotes and cells infected with parasites.

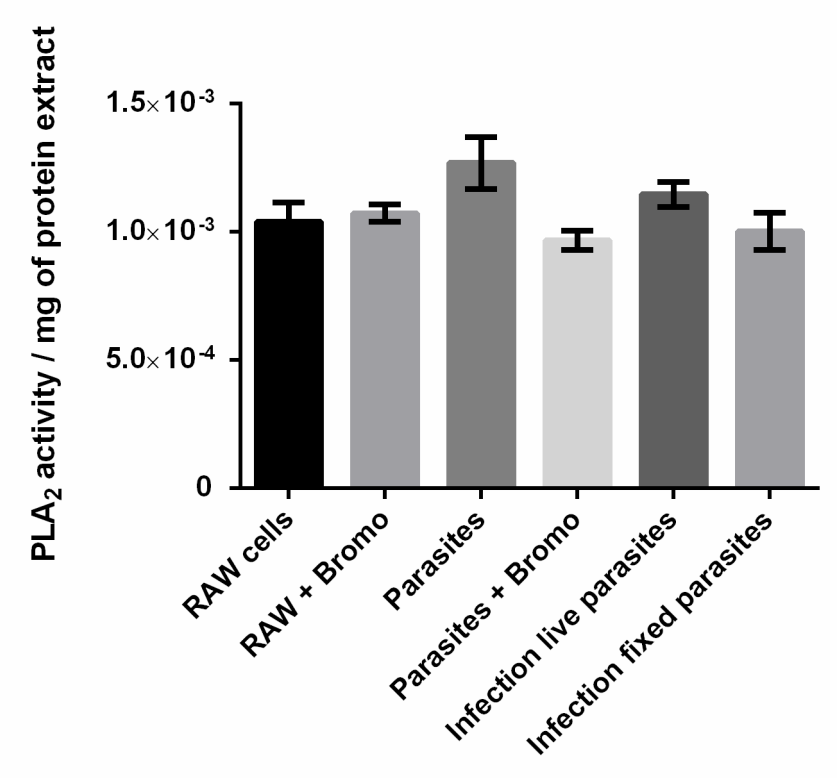

Figure 24: Evaluation of PLA_2 activity in macrophages *L. infantum* promastigotes and in infected cells. 5 x 10^6 macrophages, 5 x 10^8 promastigotes or 5 x 10^6 24 hours-exposed cells (infection ration of 10:1 parasite/cell) where sonicated in ice cold hepes buffer and the PLA_2 activity is determined for each condition as described in Material and Methods section. When indicated, 1 mM of bromoenol lactone was added to protein extract 15 min before activity determination to inhibit any secretory PLA_2 activity.

We observed that RAW cells possess noticeable PLA_2 activity that was not affected by bromoenol lactone indicating that the activity is mainly due to cytoplasmic PLA_2. In contrast, we found that detected promastigote PLA_2-like activity may result from cytosolic and secretory forms of the enzyme given that the signal is significantly lower in extracts treated with bromoenol lactone. Comparing the activities of uninfected cells, cells exposed to viable or fixed parasites we do not observed significant changes being however a slight decrease tendency detected in cells exposed to fixed parasites. These results must be interpreted with some caution: in extracts of parasite-exposed macrophages total protein concentration results from the contribution of macrophages and parasites. Given that Raw

cells and parasites have similar PLA_2 activity and the assay is performed normalizing the detected activity to the total rotein concentration of each condition, it is comprehensible that we do not observe an increased activity in infected cells. However it is expected that *in vivo*, the putative PLA_2-like enzymes of parasites will hydrolyze macrophage membrane phospholipids with possible consequences to infection.

6. Relevance of LPC to parasites infectivity

We observed that parasite-infected macrophages present high levels of LPC and that this may result from induced transcription of PLA2 and from intrinsic PLA2 activity of promastigotes. We next investigated the possible relevance of increased levels of LPC to parasite infectivity. For this we analyzed the effect in infection of OBAA, a specific PLA_2 inhibitor and of exogenous PLA_2.

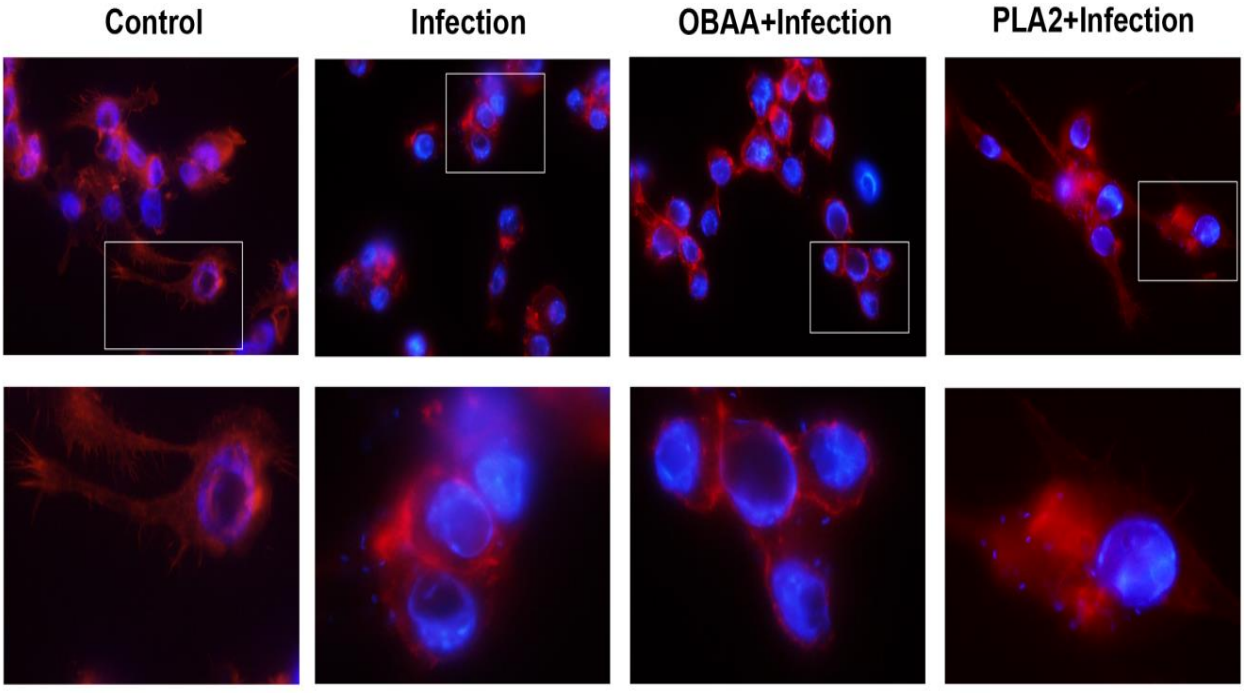

Figure 25:Relevance of PLA_2 activity and concomitant LPC formation to infectivity of *L. infantum* promastigotes. RAW cells ($4x10^4$) were were exposed for 4 hours to parasites at a 10:1 (parasite/cell) ratio. In some experiments 5 mM of the phospholipase A_2 inhibitor OBAA or exogenous PLA_2 where added to cells 1h before infection. Immunocytochemistry was performed to evaluate infection rates. Phaloidin was used to evidence F-actin (red) and DAPI to visualize cell nuclei and parasites kinetoplasts (blue). Images were obtained with a fluorescent microscope (Nikon Corporation, Japan) at 630X magnification.

We verified that inhibition of PLA_2 activity by OBBA resulted in a decrease of infected cells and in average number of parasites per cell (Figure 25). By contrast, addition of exogenous PLA_2 to cultures prior infection caused a slight increase in infected cells and a notorious increase of parasites per cell. These results strongly suggest an important role of LPC to the entry of parasites into the cells.

IV. Discussion

IV. Discussion

Innumerous studies evidence the ability of *Leishmania* parasites to actively subvert immune cells, preventing that way deleterious immune responses and allowing the perpetuation of infection (1,6,75). These studies are almost exclusive focused in host-pathogens interactions at the protein level, describing mechanisms by which parasites interfere with key proteins in macrophages, dendritic cells and neutrophils. Among such mechanisms are the cleavage of surface receptors (58), activation of phosphatases (68) and inactivation of key innate immune response-transcription factors (72). The information regarding the effects of *Leishmania* infection in host cells lipid content is in contrast very scarce. In recent years, lipids received special attention in the context of immunology, particularly because several works demonstrated that they possess important immunomodulatory functions**.** Therefore, we addressed in this work the effect of *L. infantum* promastigotes infection on macrophages phospholipid profile/metabolism and the relevance of observed changes in parasite infectivity. We observed significant alterations in the phospholipid content between uninfected cells and macrophages exposed to viable *Leishmania* promastigotes or formaldehyde fixed parasites. The most notorious alterations were observed in PC class. Infection by viable parasites caused a marked decrease in macrophage PC content with a concomitant increase in LPC class. These result are in accordance with previous observations of C. Henriques and collaborators where significantly increased levels of LPC were found in bone marrow-derived macrophage infected by *Leishmania amazonensis* (103). We also obtained interesting differences between MS spectra of the three conditions for the PC and LPC classes. Regarding PC, species with m/z values at 828.7; 832.7 and 834.7, presented a higher relative abundance in cells exposed to *Leishmania* indicating that beside the induced decrease in total PC content, parasites also cause changes in the profile of the class. Although TLC analysis only allowed the detection of LPC in lipid extracts of viable parasites-infected cells, higher sensitivity of HPLC-MS technique enabled the detection of LPC species in the three conditions analyzed. However, and supporting TLC results, LPC species remained much more abundant in macrophages exposed to viable promastigotes with species with m/z values at 568.5; 570.4 and 572.3 exclusively detected in this condition.

We showed that the observed decrease of PC and increase of LPC in promastigote-infected macrophages was in part due to an augmented transcription of cytosolic PLA_2G4F and/or to the direct activity of a *L. infantum* PLA-like enzyme. A contribution of LPC prevenient from parasite may however be also considered given that slight amounts of this lipid were detected in viable promastigotes. Although trypanosomid PLA_2 enzymes have not yet been purified and deeply characterized our hypothesis is supported by the existence of *Leishmania* genes coding putative phospholipase A_2-like proteins and by previous works where PLA_2 degrading activities were reported in *L.major* (104). The authors suggested that the putative enzymes could be involved in the biosynthesis of procyclic promastigote major surface macromolecule lipophosphoglycan. Several bacteria, viruses and protozoan parasites such as *T. cruzy* have shown to possess PLA_2-like enzymes that act as virulence factors by modifying host cell lipids (105–107). LPC was also found in saliva of parasite-vectors such as *Rhodnius prolixus*, where it acts as an antihemostatic molecule during blood feeding by preventing platelet aggregation (108). Additionally, Mesquita R.D. and collaborators demonstrated that in *Trypanosoma cruzi* infection, LPC acts as a powerful chemoattractant for monocytes at the site of the insect bite providing a continuous population of cells available for infection (109). The same group also showed that vector´s saliva LPC cause an increase in macrophage intracellular calcium levels that ultimately enhance *T.cruzy* invasion and inhibit NO production (109). In our *L.infantum*-macrophage infection model we observed that the inhibition of PLA_2 activity caused a notorious decrease in infection ratios and in contrast the addition of exogenous PLA_2 resulted in marked increase in the number of parasites per cell. Therefore, these results strongly suggest that *Leishmania*-induced LPC formation in macrophages and the direct effects of intrinsic parasite-LPC may play important roles in the installment and progression of the infection by promoting the recruitment of new macrophages and facilitating the entry of parasites into cells.

Other phospholipid classes that we found consistently altered in promastigote-infected macrophages include PS and PI. PS is an acidic natural occurring PL, which is found on the cellular membrane of a great variety of organisms. It is an essential component of biological membranes and has important regulatory functions in cells, being normally maintained in the inner leaflet of the plasma membrane. The appearance of PS on the outer leaflet of a lipid bilayer initiate several events such as platelet aggregation, cell

adhesion and is an event directly connected to cell apoptosis (110,111). The analysis of PS by HPLC-MS showed that the species with $[M-H]^-$ ions *m/z* at 760.5 and 812.5 were only detected in the control and macrophages exposed to fixed *Leishmania*. On the other hand, the $[M-H]^-$ ions at *m/z* 834.5; 836.6; and 838.5 were increased in infected macrophages, .

PIs are a group of PLs widely distributed in nature and which are involved in secretory events and in intercellular signaling. The metabolism of inositol lipids is involved in the signal transduction of many hormones, neurotransmitters and growth factors. PI classes are precursors of important signaling molecules that modulate cell growth, proliferation and death (112). The analysis of PI by HPLC-MS showed that molecular species with *m/z* at 861.6 and 887.6 were not detected in infected macrophages. Furthermore, the molecular species with *m/z* of 885.5 and 889.7 presented a lower relative abundance in infected macrophages. These results demonstrated that *Leishmania* promastigotes possess the ability to alter the PLs classes, which are essential to membrane structure and functionality (55,63).

We also analyzed the effect of infection in macrophage fatty acids profile and found that exposure to viable parasites significantly decrease cell palmitic acid (C16:0) content. Consistently, we observed a notorious increase in C18/C16 fatty acids ratio in the same condition. Finally, a slightly increased in the percentage of poly-unsaturated FAs was observed in cells infected with parasites comparing to the control. In conjunction, these results suggested an increased elongase and desaturase activity in viable promastigotes-infected cells. Although based in indirect observations, a similar hypothesis was recently formulated for *L.major* amastigotes infected dendritic cells. In the referred work, the authors performed RNA arrays and centered their analysis in lipid metabolism-related genes and found in infected cells two clusters of up regulated transcripts related to FA elongation and desaturation. To address an explanation at molecular level to our observations we analyzed by quantitative real-time RT-PCR the expression of genes coding for desaturases SCD1 and SCD2 and elongases ELOVL1, ELOVL2, ELOVL3 and ELOVL5. Neither the transcription of SCD1 or SCD2 was found to be modulated by infection, indicating that other desaturases may be involved in the observed increase of FA unsaturation. Regarding the elongases analyzed we found that the transcription of ELOVL2 was increased in macrophages exposed to viable parasites, partially justifying the

observed increase FA C18/C16 ratio in this condition. Another fact that could explain this effect and the decreased levels of palmitic acid (C16:0) registered in viable parasite infected-cells is the marked decrease in fatty acid synthase (FASN) transcription, an enzyme that catalyzes the synthesis of palmitate from acetyl-CoA and malonyl-CoA.

Among other lipid metabolism-related genes analyzed we observed that infection caused considerable alterations in the levels of FABP4 and ABCA1 mRNA. Transcription of FABP4 was shown to be unregulated, corroborating several of our results that indicate a marked modulation of FA synthesis and metabolism. Fatty acid binding protein 4 is a cytoplasmic protein that plays a central role in fatty acid uptake, transport, and metabolism (113). Its transcription is mainly regulated by peroxisome proliferator activating receptor γ (PPARγ) and therefore is plausible to speculate that infection may activate this transcription factor probably through the induction of oxidized lipids. Finally, in accordance with results from Imen Rahbi and colleagues where decreased ABCA1 mRNA levels were reported in mouse bone marrow-derived macrophages infected by *Leishmania major* (114). We observed in viable parasite infected-RAW a marked and sustained inhibition of ABCA1 transcription. The gene ABCA1 encodes for proteins related to the cholesterol efflux, which is essential to membrane dynamics and signaling cascades dependent of lipid raft formation (115). In fact, an elegant study of Rub A. and coworkers demonstrated that *Leishmania major* infection causes a depletion in macrophages membrane cholesterol which directly correlates to attenuation of CD40 transmitted signals (77).

Overall, our results indicate that *L.infantum* parasites induce marked changes in macrophage phospholipid content either through direct activity of parasite enzymes and through induced changes in host cell expression of lipid metabolism related genes. Several of these induced changes have direct consequences in parasite infectivity and should therefore be explored as possible therapeutically targets.

V. Conclusions

V. Conclusion

The general aim of the present work was to analyze the possible changes in lipidomic profile of *Leishmania infantum*-infected mouse macrophages in order to elucidate the possible contribution of lipidic changes to the pathogenesis of the infection.

Our major findings are:

- Infection causes a significant decrease in PC class and a concomitant increase in LPC class;
- This observation could be partially explained by the observed induced transcription of macrophage PLA2G4F and by the activity of a PLA_2-like enzyme of the parasite;
- Induced PLA_2 activity and/or increased levels of LPC facilitate the entry of parasites into macrophages;
- *Leishmania* promastigotes possess the ability to alter the molecular profile of PI and PS classes, which are essential to membrane structure and functionality, and are also important lipid signaling molecules;
- Infection caused a significant decrease of macrophage palmitic acid content and increase of fatty acids C18/C16 ratio;
- This effects could be explained by the observed induced transcription of macrophage elongase ELOVL2 and by a strong repression of FASN;
- Infection caused a marked decrease in the expression of cholesterol efflux transporter ABACA1, suggesting a redistribution of cellular cholesterol and alterations in membrane dynamics.

VI. References

VI. References

1. Erik Svensjö Claudia I. Brodskyn, Robson Silva, Ana Paula C.A. Lima, Verônica Schmitz, Elvira Saraiva, João B. Pesquero, Marcelo A.S. Mori, Werner Müller-Esterl, Julio Scharfstein PRB. Interplay between parasite cysteine proteases and the host kinin system modulates microvascular leakage and macrophage infection by promastigotes of the *Leishmania donovani* complex. Microbes and Infection. 2005;8:206–20.
2. L.Campino I.Franca, F.Pratlong, J.P. Dedet, T.Fiadeiro RB. Leishmaniose cutânea causada por *Leishmania infantum* zimoden mon-1. 2005;
3. Rodriguez NE, Gaur Dixit U, Allen LA, Wilson ME. Stage-specific pathways of *Leishmania infantum* chagasi entry and phagosome maturation in macrophages. PLoS One. 2011/05/10 ed. 2011;6(4):e19000.
4. Zhao C, Papadopoulou B, Tremblay MJ. *Leishmania infantum* enhances human immunodeficiency virus type-1 replication in primary human macrophages through a complex cytokine network. Clin Immunol. 2004/09/24 ed. 2004;113(1):81–8.
5. Desjeux P. Leishmaniasis Public Health Aspects and Control. Clinics itl Deunzntology. 1996;14:417–23.
6. Hsiao CH, Ueno N, Shao JQ, Schroeder KR, Moore KC, Donelson JE, et al. The effects of macrophage source on the mechanism of phagocytosis and intracellular survival of *Leishmania*. Microbes Infect. 2011/07/05 ed. 2011;13(12-13):1033–44.
7. Liese J, Schleicher U, Bogdan C. The innate immune response against *Leishmania* parasites. Immunobiology. 2008/04/15 ed. 2008;213(3-4):377–87.
8. Organization WH. Control of the leishmaniases. WHO Technical Report Series. 2010;949:202.
9. Desjeux P. Leishmaniasis: current situation and new perspectives. Comparative Immunology, Microbiology & Infectious Diseases. 2004;27:305–18.
10. Evangelos Liberopoulos, Anastazia Kei, Fotini Apostolou ME. Autoimmune manifestations in patients with visceral leishmaniasis. J Microbiol Immunol Infect. 2012/04/21 ed. 2012;
11. Frézard F Ribeiro RR DC. Pentavalent antimonials: new perspectives for old drugs. Molecules. 2009;14:2317–36.
12. DA. K. An overview of paediatric leishmaniasis. J Postgrad Med. 2003;49(1):31–8.
13. Lukasz Kedzierski Denise Bullen, Joan Curtis, Elizabeth Gardiner, Antonio Jimenez-Ruiz, and Emanuela Handman JM. A Leucine-Rich Repeat Motif of *Leishmania* Parasite Surface Antigen 2 Binds to Macrophages through the Complement receptor. The Journal of Immunology. 2004;172(8):4902–6.
14. Burton J. Bogitsh Thomas N. Oeltmann CEC, third. Human Parasitology. Elsevier; 2005.
15. Wilson R, Bates MD, Dostalova A, Jecna L, Dillon RJ, Volf P, et al. Stage-specific adhesion of *Leishmania* promastigotes to sand fly midguts assessed using an improved comparative binding assay. PLoS neglected tropical diseases. 2010 Jan;4(9):1–9.
16. Freitas VC, Parreiras KP, Duarte APM, Secundino NFC, Pimenta PFP. Development of *Leishmania (Leishmania) infantum* chagasi in its natural sandfly

vector Lutzomyia longipalpis. The American journal of tropical medicine and hygiene. 2012 Apr;86(4):606–12.
17. Louis A. Rosenthal, Fayyaz S. Sutterwala, Marcus E. Kehrli, Mosser and DM. *Leishmania major*-Human Macrophage Interactions: Cooperation between Mac-1 (CD11b/CD18) and Complement Receptor Type 1 (CD35) in Promastigote Adhesion. Infect Immun. 1996;64(6):2206–15.
18. Zufferey R, Allen S, Barron T, Sullivan DR, Denny PW, Almeida IC, et al. Ether phospholipids and glycosylinositolphospholipids are not required for amastigote virulence or for inhibition of macrophage activation by *Leishmania major*. J Biol Chem. 2003/08/29 ed. 2003;278(45):44708–18.
19. http://www.cdc.gov/parasites/leishmaniasis/biology.html.
20. Coelho-Finamore JM, Freitas VC, Assis RR, Melo MN, Novozhilova N, Secundino NF, et al. *Leishmania infantum*: Lipophosphoglycan intraspecific variation and interaction with vertebrate and invertebrate hosts. Int J Parasitol. 2010/12/02 ed. 2011;41(3-4):333–42.
21. Mahoney AB Saraiva E, Modi G, Turco SJ. SDL. Intra-species and stage-specific polymorphisms in lipophosphoglycan structure control *Leishmania donovani*-sand fly interactions. Biochemistry. 1999;38(31):9813–23.
22. Malcolm J. McConville Charles Jaffe and Pascal Schneider LFS. Structure of *Leishmania* lipophosphoglycan: inter- and intra-specific polymorphism in Old World species. Biochemistry. 1995;310:807–18.
23. McNeely TB Londner MV, Turco SJ. RG. Inhibitory effects on protein kinase C activity by lipophosphoglycan fragments and glycosylphosphatidylinositol antigens of the protozoan parasite *Leishmania*. Biochem J. 1989;259(2):601–4.
24. Desjardins M DA. Inhibition of phagolysosomal biogenesis by the *Leishmania* lipophosphoglycan. J Exp Med. 1997;185(12):2061–8.
25. Späth GF Leader B, Singer SM, Avila HA, Turco SJ, Beverley SM. EL. Lipophosphoglycan is a virulence factor distinct from related glycoconjugates in the protozoan parasite Leishmania major. Proc Natl Acad Sci U S A. 2000;97(16):9258–63.
26. Robert Lodge TOD and AD. *Leishmania donovani* lipophosphoglycan blocks NADPH oxidase assembly at the phagosome membrane. Cell Microbiol. 2006;8(12):1922–31.
27. Assis RR, Ibraim IC, Noronha FS, Turco SJ, Soares RP. Glycoinositolphospholipids from *Leishmania braziliensis* and *L. infantum*: modulation of innate immune system and variations in carbohydrate structure. PLoS Negl Trop Dis. 2012/03/06 ed. 2012;6(2):e1543.
28. Kelly A. G. Yoneyama Thais G. V. Silveira, Helio K. Takahashi, and Anita H. Straus, AKT. Characterization of *Leishmania (Viannia) braziliensis* membrane microdomains, and their role in macrophage infectivity. Journal of Lipid Research. 2006;47(10):2171–8.
29. Chawla M VRA. Alkylacylglycerolipid domain of GPI molecules of *Leishmania* is responsible for inhibition of PKC-mediated c-fos expression. J Lipid Res. 2003;44(3):594–600.
30. Souvenir D. Tachado Ralph Schawrz, Suzanna Novakovic, Malcolm McConville PG, Schofield and L. Signal transduction in macrophages by glycosylphosphatidylinositols of Plasmodium, Trypanosoma, and *Leishmania*: Activation of protein tyrosine kinases and protein kinase C by inositolglycan and diacylglycerol moieties. PNAS USA. 1997;94(8):4022–7.

31. IsabelL Merida and Glen N. Gaulton JCP. Regulation of interleukin 2-dependent growth responses by glycosylphosphatidylinositol molecules. PNAS USA. 1990;87(23):9421–5.
32. Varki A Esko JD, Freeze HH, Stanley P, Bertozzi CR, Hart GW, Etzler ME CRD. Essencial of Glycobiology. 2nd ed. Cold Spring Harbor Laboratory Press; 1999.
33. Olivier M, Atayde VD, Isnard A, Hassani K, Shio MT. *Leishmania* virulence factors: focus on the metalloprotease GP63. Microbes Infect [Internet]. 2012/06/12 ed. 2012; Available from: http://www.ncbi.nlm.nih.gov/pubmed/22683718
34. Piani A Elefanty AG, Curtis J, Handman E. IT. *Leishmania major* proteophosphoglycan is expressed by amastigotes and has an immunomodulatory effect on macrophage function. Microbes Infect. 1999;1(8):589–99.
35. Rogers ME. The role of *Leishmania* proteophosphoglycans in sand fly.pdf. Frontiers in microbiology. 2012;3:13.
36. Stierhof YD, Bates P a, Jacobson RL, Rogers ME, Schlein Y, Handman E, et al. Filamentous proteophosphoglycan secreted by *Leishmania* promastigotes forms gel-like three-dimensional networks that obstruct the digestive tract of infected sandfly vectors. European journal of cell biology. 1999 Oct;78(10):675–89.
37. Das S Remaley AT, Glew RH, Dowling JN, Kajiyoshi M, Gottlieb M. SAK. Hydrolysis of phosphoproteins and inositol phosphates by cell surface phosphatase of *Leishmania donovani*. Mol Biochem Parasitol. 1986;20(2):143–53.
38. Chaudhuri G Pan A, Chang KP. CM. Surface acid proteinase (GP63) of *Leishmania mexicana*. A metalloenzyme capable of protecting liposome-encapsulated proteins from phagolysosomal degradation by macrophages. J Biol Chem. 1989;264(13):7483–9.
39. Chen DQ Yadava N, Lu HG, Gilman-Sachs A, Peterson DA, Chang KP. KBK. Episomal expression of specific sense and antisense mRNAs in *Leishmania amazonensis*: modulation of gp63 level in promastigotes and their infection of macrophages in vitro. Infect Immun. 2000;68(1):80–6.
40. Santarém N, Racine G, Silvestre R, Cordeiro-da-Silva A, Ouellette M. Exoproteome dynamics in *Leishmania infantum*. Journal of proteomics [Internet]. Elsevier B.V.; 2013 Jun 12 [cited 2013 Jun 29];84:106–18. Available from: http://www.ncbi.nlm.nih.gov/pubmed/23558030
41. Gomez MA Hallé M, Tremblay ML, McMaster RW, Olivier M. CI. *Leishmania* GP63 alters host signaling through cleavage-activated protein tyrosine phosphatases. Sci Signal. 2009;2.
42. Gregory DJ Contreras I, Forget G, Olivier M. GM. A novel form of NF-kappaB is induced by *Leishmania* infection: involvement in macrophage gene expression. Eur J Immunol. 2008;38:10.
43. Guizani-Tabbane L Belghith M, Sassi A, Dellagi K. B-AK. *Leishmania major* amastigotes induce p50/c-Rel NF-kappa B transcription factor in human macrophages: involvement in cytokine synthesis. Infect Immun. 2004;72(5):2582–9.
44. Contreras I Nguyen O, Shio MT, McMaster RW, Olivier M. GMA. *Leishmania*-induced inactivation of the macrophage transcription factor AP-1 is mediated by the parasite metalloprotease GP63. PLoS Pathog. 2010;6:14.
45. François Chappuis Asrat Hailu, Hashim Ghalib, Suman Rijal, Rosanna W. Peeling, Jorge Alvar and Marleen Boelaert SS. Visceral leishmaniasis: what are

the needs for diagnosis, treatment and control? nature reviews | microbiology. 2007;5(11):873–82.
46. (WHO) WHO. Working to overcome the global impact of neglected tropical diseases. 2010.
47. Lenea Campino CM. Epidemiologia das Leishmanioses em Portugal. Acta Med Port. 2010;23:6.
48. Márcia J. A. Queiroz Jailson B. Correia JGBA. Visceral leishmaniasis: clinical and epidemiological features of children in an endemic area. Jornal de Pediatria. 2004;8(2):141–6.
49. Zamil J. Attar Sayda el-Safi, James Carney, Ahmed Azazy, Maha El-Hadi, Cibele Dourado, Marcel Hommel. MLC. Latex agglutination test for the detection of urinary antigens in visceral leishmaniasis. Acta Tropica. 2001;78(1):11–6.
50. Ho M Mbugua G, Wamachi A, Voller A. LJ. An enzyme-linked immunosorbent assay (ELISA) for field diagnosis of visceral leishmaniasis. The American Journal of Tropical Medicine and Hygiene. 1983;32(5):943–6.
51. Sreenivas G Singh R, Subba Raju BV, Bhatheja R, Negi NS, Salotra R. ANA. Diagnosis of visceral leishmaniasis: comparative potential of amastigote antigen, recombinant antigen and PCR. British Journal of Biomedical Science. 2002;59(4):218–22.
52. Harith AE Kager PA, Leeuwenburg J, Faber FJ, Muigai R, Kiugu S, Laarman JJ. KAH. Evaluation of a newly developed direct agglutination test (DAT) for serodiagnosis and sero-epidemiological studies of visceral leishmaniasis: comparison with IFAT and ELISA. Transactions of the Royal Society of Tropical Medicine and Hygiene. 1987;81(4):603–6.
53. Elizabeth F. Daher Michelle J.C. Oliveira, Luiz F.L.G. Franco, Jobson L. Oliveira, Geraldo B. Silva Junior, Krasnalhia Lívia S. Abreu, Guilherme A.L. Henn, Alice M.C. Martins NAR, Libório. AB. Renal Function Improvement with Pentavalent Antimonial Agents in Patients with Visceral Leishmaniasis. American journal of neuphrology. 2011;6.
54. Hall ACG and JE, saunders E. Textbook of Medical Physiology. 11th ed. 2006. p. 1152.
55. Albert L. Lehninger Michael M. Cox DLN. Lehninger Principles of Biochemistry. Fourth Edi. W. H. Freeman; 2004. p. 1124.
56. Adriana Tiscornia Maria Marquez, Ana Denicola, Otto Pritsch, Alfonso Cayota EC. Use of diaminofluoresceins to detect and measure nitric oxide in low level generating human immune cells. Journal of Immunological Methods. 2008;342:9.
57. Wright SD SSC. Receptors for C3b and C3bi promote phagocytosis but not the release of toxic oxygen from human phagocytes. J Exp Med. 1983;158(6):2016–23.
58. Mosser DM EPJ. The third component of complement (C3) is responsible for the intracellular survival of *Leishmania* major. Nature. 1987;327:329–31.
59. RS. B. *Leishmania mexicana mexican*a: attachment and uptake of promastigotes to and by macrophages in vitro. J Protozool. 1983;30(2):314–22.
60. Culley FJ Kaye PM, McAdam KP, Raynes JG. HRA. C-reactive protein binds to a novel ligand on *Leishmania donovani* and increases uptake into human macrophages. J Immunol. 1996;156(12):4691–6.
61. Wilson ME PRD. Evidence that *Leishmania donovani* utilizes a mannose receptor on human mononuclear phagocytes to establish intracellular parasitism. J Immunol. 1986;136(12):4681–8.

62. Rawlings JS Harrison DA. RKM. The JAK/STAT signaling pathway. J Cell Sci. 2004;117:1281–3.
63. Xie QW Nathan C. WR. Promoter of the mouse gene encoding calcium-independent nitric oxide synthase confers inducibility by interferon gamma and bacterial lipopolysaccharide. J Exp Med. 1993;177(6):1779–84.
64. Nandan D RNE. Attenuation of gamma interferon-induced tyrosine phosphorylation in mononuclear phagocytes infected with *Leishmania donovani:* selective inhibition of signaling through Janus kinases and Stat1. Infect Immun. 1995;63(11):4495–500.
65. Blanchette J Faure R, Siminovitch KA, Olivier M. RN. *Leishmania*-induced increases in activation of macrophage SHP-1 tyrosine phosphatase are associated with impaired IFN-gamma-triggered JAK2 activation. Eur J Immunol. 1999;29(11):3737–44.
66. Gui-Jie Feng Margaret M. Harnett, Xiao-Qing Wei, Andrei V. Nikolaev, Adrian P. Higson, and Foo-Y. Liew HSG. Extracellular Signal-Related Kinase (ERK) and p38 Mitogen-Activated Protein (MAP) Kinases Differentially Regulate the Lipopolysaccharide-Mediated Induction of Inducible Nitric Oxide Synthase and IL-12 in Macrophages: *Leishmania* Phosphoglycans Subvert Macr. The Journal of Immunology. 1999;163(12):6403–12.
67. Olivier M Reiner NE. BRW. Defective stimulus-response coupling in human monocytes infected with *Leishmania donovani* is associated with altered activation and translocation of protein kinase C. Proceedings of the National Academy of Sciences. 1992;89(16):7481–5.
68. Marina Tiemi Shio Amandine Isnard, Benjamin Ralph, Irazu Contreras, Maria Adelaida Gomez, Issa Abu-Dayyeh, andMartin Olivierv KH. Host Cell Signalling and *Leishmania* Mechanisms of Evasion. Journal of tropical medicine. 2012;14.
69. Simoncic PD Barber DL, Tremblay ML, McGlade CJ. L-LA. The T cell protein tyrosine phosphatase is a negative regulator of janus family kinases 1 and 3. Curr Biol. 2002;12(6):446–53.
70. Ten Hoeve J Fu Y, Zhu W, Tremblay M, David M, Shuai K. de JI-SM. Identification of a nuclear Stat1 protein tyrosine phosphatase. Mol Cell Biol. 2002;22(16):5662–8.
71. Forget G Brochu S, Rivest S, Radzioch D, Olivier M. SKA. Role of host phosphotyrosine phosphatase SHP-1 in the development of murine leishmaniasis. Eur J Immunol. 2001;31(11):3185–96.
72. Teresa C. Calegari-Silva Luiz Dione Barbosa De-Melo, Elvira M. Saraiva, Deivid C. Soares, Maria Bellio, Ulisses G. Lopes RMSP. NF-kB-mediated repression of iNOS expression in *Leishmania amazonensis* macrophage infection. Immunology Letters. 2009;127(1):19–26.
73. Lamia Guizani-Tabbane Meriam Belghith, Atfa Sassi, and Koussay Dellagi KB-A. *Leishmania major* Amastigotes Induce p50/c-Rel NF-κB Transcription Factor in Human Macrophages: Involvement in Cytokine Synthesis. Infect Immun. 2004;75(5):2582–9.
74. Rodrigues MZ Mehta S, Zhang XQ, Gois LL, Schooley RT, Badaro R. GMF. Th1/Th2 cytokine profile in patients coinfected with HIV and *Leishmania* in Brazil. Clin Vaccine Immunol. 2011;18(10):1765–9.
75. Carrera L Badolato R, Hieny S, Muller W, Kuhn R, Sacks DL. GRT. *Leishmania* promastigotes selectively inhibit interleukin 12 induction in bone marrow-

derived macrophages from susceptible and resistant mice. J Exp Med. 1996;182(2):515–26.
76. Reiner NE Wilson CB, McMaster WR, Burchett SK. NW. Modulation of in vitro monocyte cytokine responses to *Leishmania donovani*. Interferon-gamma prevents parasite-induced inhibition of interleukin 1 production and primes monocytes to respond to *Leishmania* by producing both tumor necrosis factor-alpha and in. J Clin Invest. 1990;85(6):1914–24.
77. Rub A, Dey R, Jadhav M, Kamat R, Chakkaramakkil S, Majumdar S, et al. Cholesterol depletion associated with *Leishmania major* infection alters macrophage CD40 signalosome composition and effector function. Nat Immunol [Internet]. 2009/02/10 ed. 2009;10(3):273–80. Available from: http://www.ncbi.nlm.nih.gov/pubmed/19198591
78. Vidalain PO Servet-Delprat C, Rabourdin-Combe C, Gerlier D, Manié S. AO. CD40 signaling in human dendritic cells is initiated within membrane rafts. EMBO J. 2000;19(13):3304–13.
79. Rabhi I, Rabhi S, Ben-Othman R, Rasche A, Consortium S, Daskalaki A, et al. Transcriptomic signature of *Leishmania* infected mice macrophages: a metabolic point of view. PLoS Negl Trop Dis [Internet]. 2012/08/29 ed. 2012;6(8):e1763. Available from: http://www.ncbi.nlm.nih.gov/pubmed/22928052
80. Kai Zhang David A. Scott, Roberto Docampo, John Turk and Stephen M. Beverley F-FH. *Leishmania* salvage and remodelling of host sphingolipids in amastigote survival and acidocalcisome biogenesis. Molecular Microbiology. 2005;55(5):1566–78.
81. Maroun Bou Khalil Hu Zhou, Fred Elisma, Leigh Anne Swayne, Alexandre P. Blanchard, Zemin Yao, Steffany A.L. Bennett, and Daniel Figeys WH. Lipidomics Era: Accomplishments and Challenges. Mass Spectrometry Reviews. 2010;29(6):877–929.
82. Hayder Z. Ali CRH and PD. Endocytosis and Sphingolipid Scavenging in *Leishmania mexicana* Amastigotes. Biochem Res Int. 2012;8.
83. Zhang O Balakrishna Pillai A, Zhang K. XW. Developmentally regulated sphingolipid degradation in *Leishmania major*. PLoS One. 2012;7:10.
84. Sanjukta Ghosh Sonali Das, Sanghamitra Raha, Nilanjana Maulik, Dipak K. Das, Syamal Roy and Subrata Majumdar SB. Generation of ceramide in murine macrophages infected with *Leishmania donovani* alters macrophage signaling events and aids intracellular parasitic survival. Molecular and Cellular Biochemistry. 2001;223(2):47–60.
85. Zhang O Xu W, Hsu FF, Turk J, Kuhlmann FM, Wang Y, Soong L, Key P, Beverley SM, Zhang K. WMC. Degradation of host sphingomyelin is essential for *Leishmania* virulence. PLoS Pathog. 2009;5.
86. Ghosh S Das S, Raha S, Maulik N, Das DK, Roy S, Majumdar S. BS. Generation of ceramide in murine macrophages infected with *Leishmania donovani* alters macrophage signaling events and aids intracellular parasitic survival. Mol Cell Biochem. 2001;223(2):47–60.
87. Perera R, Riley C, Isaac G, Hopf-Jannasch AS, Moore RJ, Weitz KW, et al. Dengue virus infection perturbs lipid homeostasis in infected mosquito cells. PLoS Pathog. 2012/03/30 ed. 2012;8(3):e1002584.
88. Deborah L. Diamond Jon M. Jacobs, Christina M. Sorensen, Kathie-Anne Walters, Sean C. Proll, Jason E. McDermott, Marina A. Gritsenko, Qibin Zhang, Rui Zhao, Thomas O. Metz, David G. Camp II, Katrina M. Waters, Richard D. Smith, Charles M. Rice and Michae AJS. Temporal Proteome and Lipidome

Profiles Reveal Hepatitis C Virus-Associated Reprogramming of Hepatocellular Metabolism and Bioenergetics. PLoS Pathog. 2010;6:18.
89. Chunxiu Hu MeiWang, Jan van der Greef, Thomas Hankemeier, Guowang Xu R van der H. Analytical strategies in lipidomics and applications in disease biomarker discovery. Journal of Chromatography B. 2009;877(26):2836–46.
90. Santinha DR Maciel EA, Simões CS, Rosa S, Neves BM, Macedo B, Domingues P, Cruz MT, Domingues MR. MDR. Profiling changes triggered during maturation of dendritic cells: a lipidomic approach. Anal Bioanal Chem. 2012;403(2):457–71.
91. SK P. Dissecting lipid raft facilitated cell signaling pathways in cancer. Biochim Biophys Acta. 2008;1785(2):182–206.
92. Piomelli D Rapaka R. AG. A neuroscientist's guide to lipidomics. Nat Rev Neurosci. 2007;8(10):743–54.
93. Emilie Layre DBM. Lipidomic profiling of model organisms and the world's major pathogens. Biochimie. 2012;(1):109–15.
94. Yang K, Han X. Accurate quantification of lipid species by electrospray ionization mass spectrometry - Meet a key challenge in lipidomics. Metabolites. 2012/08/21 ed. 2011;1(1):21–40.
95. Oresic M Vidal-Puig A. HVA. Lipidomics: a new window to biomedical frontiers. Trends Biotechnol. 2008;26(12):647–52.
96. Wolf C QPJ. Lipidomics: practical aspects and applications. Prog Lipid Res. 2008;47(1):15–36.
97. Zheng Cui MJT. Phospholipid profiling by tandem mass spectrometry. Journal of Chromatography B. 2007;877(26):2709–15.
98. BLIGH EG DW. A rapid method of total lipid extraction and purification. Can J Biochem Physiol. 1959;37(8):911–7.
99. Bartlett EM LD. Spectrophotometric determination of phosphate esters in the presence and absence of orthophosphate. Anal Biochem. 1970;36:159–67.
100. Sabria Aued-Pimentel, João Henrique Ghilardi Lago MHC, Kumagai EE. Evaluation of a methylation procedure to determine cyclopropenoids fatty acids from Sterculia striata St. Hil. Et Nauds seed oil. Journal of chromatography. A. 2004;1054(1-2):235–9.
101. Schwalbe-Herrmann M, Willmann J, Leibfritz D. Separation of phospholipid classes by hydrophilic interaction chromatography detected by electrospray ionization mass spectrometry. Journal of chromatography. A [Internet]. Elsevier B.V.; 2010 Aug 6 [cited 2013 Mar 19];1217(32):5179–83. Available from: http://www.ncbi.nlm.nih.gov/pubmed/20598701
102. Pulfer M, Murphy RC. Electrospray mass spectrometry of phospholipids. Mass spectrometry reviews. 2003;22(5):332–64.
103. Henriques C, Atella GC, Bonilha VL, De Souza W. Biochemical analysis of proteins and lipids found in parasitophorous vacuoles containing *Leishmania amazonensis*. Parasitology research. 2003 Jan;89(2):123–33.
104. Smith TK, Milne FC, Sharma DK, Crossman A, Brimacombe JS, Ferguson M a. Early steps in glycosylphosphatidylinositol biosynthesis in Leishmania major. The Biochemical journal. 1997 Sep 1;326 (Pt 2:393–400.
105. Sitkiewicz I, Stockbauer KE MJ. Secreted bacterial phospholipase A2 enzymes: better living through phospholipolysis. Trends Microbiol. 2007;15(2):63–9.
106. Heffernan BJ, Thomason B, Herring-Palmer A, Shaughnessy L, McDonald R, Fisher N, Huffnagle GB HP. *Bacillus anthracis* phospholipases C facilitate

macrophage-associated growth and contribute to virulence in a murine model of inhalation anthrax. Infect Immun. 2006;74(7):3756–64.
107. Matte C, Maion G, Mourad W, Olivier M. *Leishmania donovani*-induced macrophages cyclooxygenase-2 and prostaglandin E2 synthesis. Parasite immunology. 2001 May;23(4):177–84.
108. Golodne DM, Monteiro RQ, Graca-Souza A V, Silva-Neto M a C, Atella GC. Lysophosphatidylcholine acts as an anti-hemostatic molecule in the saliva of the blood-sucking bug *Rhodnius prolixus*. The Journal of biological chemistry. 2003 Jul 25;278(30):27766–71.
109. Mesquita RD, Carneiro AB, Bafica A, Gazos-Lopes F, Takiya CM, Souto-Padron T, et al. *Trypanosoma cruzi* infection is enhanced by vector saliva through immunosuppressant mechanisms mediated by lysophosphatidylcholine. Infection and immunity. 2008 Dec;76(12):5543–52.
110. Leventis PA GS. The distribution and function of phosphatidylserine in cellular membranes. Annu Rev Biophys. 2010;39:407–27.
111. Maciel E, Da Silva RN, Simões C, Domingues P, Domingues MRM. Structural characterization of oxidized glycerophosphatidylserine: evidence of polar head oxidation. Journal of the American Society for Mass Spectrometry. 2011 Oct;22(10):1804–14.
112. Hsu FF TJ. Characterization of phosphatidylinositol, phosphatidylinositol-4-phosphate, and phosphatidylinositol-4,5-bisphosphate by electrospray ionization tandem mass spectrometry: a mechanistic study. J Am Soc Mass Spectrom. 2000;11(11):986–99.
113. Hu W, Zhou X, Jiang M, Duan Y, Chen Y, Li X, et al. Statins synergize dexamethasone-induced adipocyte fatty acid binding protein expression in macrophages. Atherosclerosis. Elsevier Ireland Ltd; 2012 Jun;222(2):434–43.
114. Imen Rabhi Rym Ben-Othman, Axel Rasche, Sysco Consortium, Adriani Daskalaki, Bernadette Trentin, David Piquemal, Béatrice Regnault, Albert Descoteaux, Lamia Guizani-Tabbane SR. Transcriptomic Signature of *Leishmania* Infected Mice Macrophages: A Metabolic Point of View. PLoS Negl Trop Dis. 2012;6:11.
115. Zhang L, Jiang M, Shui Y, Chen Y, Wang Q, Hu W, et al. DNA topoisomerase II inhibitors induce macrophage ABCA1 expression and cholesterol efflux-An LXR-dependent mechanism. Biochimica et biophysica acta. Elsevier B.V.; 2013 Jun;1831(6):1134–45.